Fractal features of Surface Electromyogram: A new measure for low level muscle activation

A thesis submitted in fulfilment
of the requirements for the degree of

Doctor of Philosophy

Sridhar Poosapadi Arjunan

M.E.(Communication Systems Engineering)

School of Electrical and Computer Engineering
Science, Engineering and Technology Portfolio
RMIT University
August 2008

Declaration

I certify that except where due acknowledgements has been made, the work is that of the author alone; the work has not been submitted previously, in whole or in part, to qualify for any other academic award; the content of the thesis is the result of work which has been carried out since the official commencement date of the approved research program; and, any editorial work, paid or unpaid, conducted by a third party is acknowledged; and, ethics procedures and guidelines have been followed.

Sridhar Poosapadi Arjunan

Acknowledgements

I would like to thank my supervisor, Asso. Prof. Dr. Dinesh Kant Kumar for his constant support and excellent guidance during the course of this research. He gave me good inspiring ideas and guidance every time on how to start and pursue my research. He as a mentor helped me to proceed in a right direction in research. His motivation helped me to come up with a good research proposal and to build my own confidence in preparation of my study.

I would like to extend my most sincere thanks to Prof. Dr. Hans Weghorn for his support and supervision during my research placement in BA-University of Cooperative Education, Stuttgart, Germany for 6 months. I would also like to thank Prof. Tzyy Ping Jung, Swartz Center for Computational Neuroscience Institute for Neural Computation, University of California, San Diego for helping and providing me with the EEG data for my research work.

My heartfelt thanks to my colleagues Wai Chee, Ganesh, Ivan, and Vijay for providing constant help with a fun and inspiring environment in the research office. I would like to express my deepest gratitude to my father Mr. D. Arjunan, my mother Mrs. A. Dhanalakshmi, my father-in-law Mr. N. Ravisankar and my brother Sasikumar for their constant support throughout my study and life. Last but not least, my grateful thanks to my wife Priyavardhini and my cute daughter Shamitha for their love and understanding during my research study.

Finally, i would like to thank the School of Electrical and Computer Engineering, RMIT University, Australia, for providing me with scholarship during my research study.

Abstract

Identifying finger and wrist flexion based actions using single channel surface electromyogram have a number of rehabilitation, defence and human computer interface applications. These applications are currently infeasible because of unreliability in classification of sEMG when the level of muscle contraction is low and when there are multiple active muscles. The presence of noise and cross-talk from closely located and simultaneously active muscles is exaggerated when muscles are weakly active such as during maintained wrist and finger flexion. It has been established in literature that surface electromyogram (sEMG) and other such biosignals are fractal signals. Some researchers have determined that fractal dimension (FD) is related to strength of muscle contraction. On careful analysis of fractal properties of sEMG, this research work has established that FD is related to the muscle size and complexity and not to the strength of muscle contraction.

The work has also identified a novel feature, maximum fractal length (MFL) of the signal, as a good measure of strength of contraction of the muscle. From the analysis, it is observed that while at high level of contraction, root mean square (RMS) is an indicator of strength of contraction of the muscle, this relationship is not very strong when the

muscle contraction is less than 50% maximum voluntary contraction. This work has established that MFL is a more reliable measure of strength of contraction compared to RMS, especially at low levels of contraction.

This research work reports the use of fractal properties of sEMG to identify the small changes in strength of muscle contraction and the location of the active muscles. It is observed that fractal dimension (FD) of the signal is related with the properties of the muscle while maximum fractal length (MFL) is related to the strength of contraction of the associated muscle. The results show that classifying MFL and FD of a single channel sEMG from the forearm it is possible to accurately identify a set of finger and wrist flexion based actions even when the muscle activity is very weak. It is proposed that such a system could be used to control a prosthetic hand or for human computer interface.

Publications Arising From This Thesis

Book Chapter

1. **Sridhar P. Arjunan**, Hans Weghorn, Dinesh K. Kumar, & Wai C. Yau. Silent Bilingual Vowel Recognition - Using fSEMG for HCI based Speech Commands. *The Enterprise Information Systems IX book, Lecture Notes in Business Information Processing, 12,* 366-378, Springer, 2009.

Fully Refereed International Journals

1. **Sridhar P. Arjunan** & Dinesh K. Kumar (2008). Identification of finger and Wrist Flexion Using Fractal Properties of Surface Electromyogram. *Journal of Neuro Engineering and Rehabilitation.* Biomed Central. *(Under Review)*
2. **Sridhar P. Arjunan** & Dinesh K. Kumar (2008). Fractal analysis of Surface Electromyogram; A new measure for low - level muscle activation *Journal of Electromyography and kinesiology.* Elsevier. *(Submitted)*
3. Wai C. Yau, Dinesh K. Kumar, Hans Weghorn & **Sridhar P. Arjunan** (2008). Visual speech recognition using dynamic features and support vector machines. *International Journal of Image and Graphics, 8*(3),419-437, World Scientific.
4. Ganesh R. Naik, Dinesh K. Kumar, M. Palaniswami & **Sridhar P. Arjunan** (2008). Independent component approach to the analysis of Hand gesture sEMG and Facial sEMG. *Biomedical Engineering: Applications, Basis and Communications (BME), 20* (2), 83-93, World Scientific.

5. Wai C. Yau, Dinesh K. Kumar, & **Sridhar P. Arjunan** (2007). Visual recognition of speech consonants using facial movement features.*Integrated Computer-Aided Engineering, 14*(1),49-61, IOS Press.

6. D. Djuwari, Dinesh K. Kumar, Ganesh R. Naik, & **Sridhar P. Arjunan** (2007). Limitations and applications of ICA for Surface Electromyogram-validation for identifying hand gestures. *Special Issue on Biomedical Signal Sensing and Intelligent Information Processing, International journal of Computational Intelligence and Applications (IJCIA),* World Scientific, *(Accepted - In Press)*

7. D. Djuwari, Dinesh K. Kumar, Ganesh R. Naik, M. Palaniswami & **Sridhar P. Arjunan** (2006). Limitations and applications of ICA for surface electromyogram. *Journal of Electromyography and Clinical Neurophysiology, 46*(5), 295-309, Belgium.

Fully Refereed Conference Proceedings

1. **Sridhar P. Arjunan**, & Dinesh K. Kumar (2008). Identification of Muscle Properties Using Fractal Analysis of sEMG signal. *19th EURASIP international conference BIOSIGNAL 2008,* June 29 - July 1, Brno, Czech Republic.

2. **Sridhar P. Arjunan**, Dinesh K. Kumar, & Tzzy-Ping Jung (2008). Fractal based method for alertness measurement using EEG. *14th Annual Meeting of the Organization for Human Brain Mapping, NeuroImage,* Vol. 41, Sup. 1, June 15-19, Melbourne, Australia.

3. **Sridhar P. Arjunan**, & Dinesh. K. Kumar (2008). Fractal features based technique to identify subtle forearm movements and to measure alertness using Physiological signals (sEMG, EEG). *IEEE Region 10 Conference - TENCON 2008,* Nov. 19-21, Hyderabad, India (Accepted) .

4. Wai C. Yau, **Sridhar P. Arjunan**, & Dinesh. K. Kumar (2008). Classification of Voiceless Speech Using Facial Muscle Activity and Vision based Techniques. *IEEE Region 10 Conference - TENCON 2008,* Nov. 19-21, Hyderabad, India (Accepted).
5. Ganesh R. Naik, Dinesh K. Kumar, & **Sridhar P. Arjunan** (2008). Reliability of Facial Muscle Activity to Identify Vowel Utterance. *IEEE Region 10 Conference - TENCON 2008,* Nov. 19-21, Hyderabad, India (Accepted).
6. Ganesh R. Naik, Dinesh K. Kumar, & **Sridhar P. Arjunan** (2008). Multi modal gesture identification for HCI using surface EMG. *ACM MindTrek International conference,* Oct. 7-9, Tampere, Finland (Accepted).
7. **Sridhar P. Arjunan**, & Dinesh K Kumar (2007). Fractal Based Modelling and Analysis of Electromyography (EMG) To Identify Subtle Actions. *29th Annual International Conference of the IEEE Engineering in Medicine and Biology Society,* Aug. 23-26, Lyon, France.
8. **Sridhar P. Arjunan**, & Dinesh K Kumar (2007). Fractal theory based Non-linear analysis of sEMG. *The Third International Conference on Intelligent Sensors, Sensor Networks and Information Processing(ISSNIP),* Dec. 3-6, Melbourne, Australia.
9. **Sridhar P. Arjunan**, Hans Weghorn, Dinesh K. Kumar, & Wai C. Yau (2007). Silent bilingual vowel recognition - Using fSEMG for HCI based speech command. *Int. Conf. on Enterprise Information Systems(ICEIS),* Vol. 5, pp. 68-75, June, Funchal, Portugal. **(Best Paper Award)**
10. **Sridhar P. Arjunan**, & Dinesh K Kumar (2007). Recognition of Facial Movements and Hand Gestures Using Surface Electromyogram(sEMG) for HCI Based Applications. *9th Biennial Conference of the Australian Pattern Recognition Society on Digital Image Computing Techniques and Applications (DICTA),* pp. 1-6, Dec 3-5, Adelaide, Australia.

11. Ganesh. R. Naik, Dinesh K. Kumar, Hans Weghorn, **Sridhar P. Arjunan**, & M. Palaniswami (2007). Limitations and Applications of ICA in Facial sEMG and Hand Gesture sEMG for Human Computer Interaction. *9th Biennial Conference of the Australian Pattern Recognition Society on Digital Image Computing Techniques and Applications (DICTA),* pp. 1-6, Dec 3-5, Adelaide, Australia.
12. **Sridhar P. Arjunan**, Hans Weghorn, Dinesh K. Kumar, & Wai C. Yau (2006). Vowel recognition of English and German language using facial movement(SEMG) for speech control based HCI. *HCSNet Workshop on the Use of Vision in HCI (VisHCI),* Vol. 56, pp. 13-18, Nov. 1-3, Canberra, Australia.
13. **Sridhar P Arjunan**, Dinesh K. Kumar, Wai C. Yau, & Hans Weghorn (2006). Unspoken Vowel Recognition Using Facial Electromyogram. *28th IEEE EMBS Annual International Conference,* pp. 2191 - 2194, Aug. 30 - Sep. 3, New York, USA.
14. **Sridhar P. Arjunan**, Dinesh K. Kumar, Wai C. Yau, & Hans Weghorn (2006). Facial SEMG for speech recognition - inter subject variation. *Workshop on Bio-signal processing and classfication at International Conference on Informatics in Control, Automation and Robotics,* pp. 3-12, Aug. 1-5, Setubal, Portugal.
15. **Sridhar P. Arjunan**, Dinesh K. Kumar, Wai C. Yau, & Hans Weghorn (2006). Unvoiced speech control based on vowels detected by facial surface electromyogram. *IADIS International Conference E-society,* Vol.1, pp. 381-388, July 13-16, Dublin, Ireland. **(Outstanding Paper award)**
16. Wai C. Yau, Dinesh K. Kumar, **Sridhar P. Arjunan** & S. Kumar (2006). Visual speech recognition using wavelet transform and moment based features. *International Conference on Informatics in Control, Automation and Robotics,* pp. 340-345, Aug. 1-5, Setubal, Portugal.
17. Wai C. Yau, Dinesh K. Kumar, & **Sridhar P. Arjunan** (2006).

Visual speech recognition method using translation, scale and rotation invariant features. *IEEE International Conference on Advanced Video and Signal based Surveillance,* pp. 63, Nov. 22-24, Sydney, Australia.

18. Wai C. Yau, Dinesh K. Kumar, & **Sridhar P. Arjunan** (2006). Voiceless speech recognition using dynamic visual speech features. *HCSNet Workshop on the Use of Vision in HCI (VisHCI)*, Vol. 56, pp. 93-101, Nov. 1-3, Canberra, Australia.

19. Wai C. Yau, Dinesh K. Kumar, **Sridhar P. Arjunan**, & S. Kumar (2006). Visual speech recognition using image moments and multiresolution wavelet images. *International Conference on Computer Graphics, Imaging and Visualisation,* pp. 194-199, July 25-28, Sydney, Australia.

20. Ganesh. R. Naik, Dinesh K. Kumar, **Sridhar P. Arjunan**, & M. Palaniswami (2006). Limitations and Applications of ICA for Surface Electromyogram. *IEEE International Conference of the Engineering in Medicine and Biology Society (EMBS),*pp. 5739–5742, Aug. 30 - Sep. 3, New York, USA.

21. Ganesh. R. Naik, Dinesh K. Kumar, **Sridhar P. Arjunan**, & M. Palaniswami (2006). ICA for Surface Electromyogram. *Workshop on Biosignal Processing and Classification at International Conference on Informatics in Control, Automation and Robotics,* pp. 3-12, Aug. 1-5, Setubal, Portugal.

Contents

List of Figures

List of Tables

Chapter 1

Introduction

1.1 Introduction

Prosthetic control and a number of other rehabilitation and defence applications require automated identification of hand movement and gesture. A simple representation of robotic hand movement is shown in Fig.1.1. One method to determine the movement and posture is by estimating the strength of contraction of associated muscles based on the electrical activity of the muscles. Surface electromyography (sEMG) (Basmajian and De Luca, 1985) is a non-invasive, easy to record electrical activity of skeletal muscle recorded from the skin surface. sEMG has several advantages compared with the invasive electromyography recording. SEMG is recorded using surface electrodes that are placed on the surface of the skin and is the result of large number of muscle activities contaminated by noises and artefacts. It is a complex signal and lacks muscle selectivity.

Classification of sEMG with movement and gesture is a desired option (Englehart and Hudgins, 2003; Momen et al., 2007) but is not simple when there are

Figure 1.1: Representation of a robotic hand control [Source: Shadow Robot Company Ltd.(ShadowRobot, 2008)]

number of simultaneously active muscles and when the muscle activity is weak such as during finger and wrist flexion and extension. While there are reported works (Crawford et al., 2005; Nagata et al., 2005) where multiple channels of sEMG have been used for identifying actions such as finger and wrist flexion and extension, these require precise location of the electrodes and the system needs to be calibrated for each experiment.

Recent work (Momen et al., 2007) has reported on the use of two channel sEMG to identify the user defined actions but conducting similar experiments indicates that such a technique is unsuitable for predefined hand gestures and requires the system to be trained for each session. There is a need for a simple and reliable system that

- does not require large number of electrodes,

- is easy to use, and
- does not require to be trained for each session.

A strong relationship exists between the magnitude and spectral features of sEMG with the force of muscle contraction (Basmajian and De Luca, 1985; Cram et al., 1998). Various analogous measures such as root mean square (RMS), integral of the signal, auto-regression, and wavelet coefficients have been used to classify the signal against the desired movement and/or posture (Christodoulou and Pattichis, 1999; Coatrieux et al., 1983; Englehart and Hudgins, 2003; Kumar and Pah, 2000; Ren et al., 2006). The classification of these features has been achieved using a range of parametric and non-parametric techniques, ranging from Bayesian statistical classifiers; neural networks (Kumar et al., 2001; Ren et al., 2006) and a predictive approach (Coatrieux et al., 1983). The issues for classifying sEMG to identify actions are:

- reliability,
- reduction in the number of electrodes or channels, insensitivity to placement of electrodes for recording, and
- identification of complex actions such as finger and wrist flexions.

The fundamental principle of motor unit action potential (MUAP) density based techniques reported in literature (Kleine et al., 2007; Sandbrink and Culcea, 2002; Zhou et al., 2001) is that these are based on shape matching and are suitable for identifying MUAP of a predefined shape. Strategies used include template matching (Katsis et al., 2007; Zhou and Rymer, 2007), use of neural networks (Christodoulou and Pattichis, 1999; Coatrieux et al., 1983; Kumar

et al., 2001) and wavelets decomposition (Ren et al., 2006). Such systems are sensitive to shape of the MUAP. The variation of the shape of MUAP originating from different muscles due to difference in the conduction pathways makes these techniques unsuitable when there are multiple active muscles. Another proposed measure of strength of muscle activity from sEMG is fractal dimension (FD) (Anmuth et al., 1994; Gitter and Czerniecki, 1995; Gupta et al., 1997; Hu et al., 2005). While researchers have attempted to study the relationship between FD and muscle activity, this relationship does not appear to be well understood.

1.2 Problem statement

One general limitation of the techniques mentioned in the previous section is that these techniques are unreliable at low levels of contraction. This is because the relationship between sEMG and the force of contraction is not linear at low levels of sEMG (Basmajian and De Luca, 1985; Kleine et al., 2007) and at a low level of contraction, the signal to noise ratio for sEMG is very poor. Due to this, it is difficult to automatically segment the signal activity from the background activity (Gazzoni et al., 2004). While statistical techniques are suitable where muscle activity is large, manual intervention is required when muscle activity is small.

The other difficulty when using sEMG to identify complex actions such as wrist and finger flexion is the necessity to map sEMG signals corresponding to the relative contraction of different muscles (Duchêne and Goubel, 1993; Gazzoni et al., 2004). With RMS or other magnitude based features, this either requires an array of electrodes (Crawford et al., 2005; Nagata et al., 2005) or the system

needs to be trained for individual experiments (Cram et al., 1998; Gazzoni et al., 2004), making it unsuitable for lay users and for people with amputations.

In particular, isometric steady-state contraction of an individual muscle is proportional to the force produced by the muscle. However, this relationship changes significantly with change in the shape of the muscle, fatigue in a muscle, noise etc. It is also very difficult to isolate activity from a single muscle using noninvasive surface measurements. Decoding the wrist or finger flexion using sEMG signals is a challenging task.

With the need for identifying complex and subtle actions and gestures, nonlinear methods are emerging to characterize sEMG. The nonlinear properties may be estimated by calculating nonlinear measures such as entropies, correlation and fractal dimensions, and self-correlation (Nussbaum, 2006). This thesis reports research where fractal properties of sEMG have been analysed to determine features that can be used to identify different actions.

1.3 Research Aim and Objectives

The main aim of this research is to investigate fractal based features for identification of subtle (wrist and finger) movements or gestures using single channel recording of sEMG. The objectives of this research work are to:

- analyse the efficacy of Fractal dimension (FD) of sEMG, as a measure of the property (complexity) of the muscles.
- compute and analyse the new fractal feature, Maximum Fractal Length (MFL) of sEMG, as a measure of low-level muscle activity at different force

levels of muscle activation.

- examine the applications of these fractal feature set (FD, MFL) in wrist & finger movement identification using single channel sEMG.
- test the efficacy of these features for the application to Electroencephalography (EEG).

This thesis reports the use of fractals to measure the properties of the sEMG signal. This research investigates the evaluation of the relationship between levels of muscle contraction, size of muscles and depth of the active muscle on the fractal properties (Fractal dimension) of sEMG. This research has also identified a new fractal feature, Maximum fractal length (MFL), as a measure of low-level muscle activity. The MFL is the fractal logarithmic length of sEMG at the lowest scale and relates to the small changes in the subtle muscle activity.

The main advantages of using these fractal features of sEMG in identification of the subtle movements are:

(i) retrieve information pertaining to the physiological properties of muscle, at different force levels of muscle contraction,

(ii) able to identify the small changes in the low-level muscle activation and

(iii) less sensitive to background noise and thus inter-experimental variation.

1.4 Outline of the thesis

The thesis on this research study is organized into eight chapters. The *first chapter* presents an introduction to the research work.

Chapter 2 provides an overview of the related work and literature studies on the sEMG based feature extraction and classification methods for identification of human movements.

Chapter 3 explains the generation of sEMG, factors that influence the sEMG and its applications in various fields.

Chapter 4 covers the fundamental concepts of fractals and its properties. This chapter explains the concept of self-similarity and fractal dimension, as an index of self-similar property. Also, it presents the algorithm for computation of fractal dimension.

Chapter 5 describes the fractal analysis of sEMG for feature extraction. This chapter presents a method for computation of fractal features and their relation to the properties and activation of muscle.

Chapter 6 reports on the results from the experimental analysis in evaluating the performance of fractal features (FD, MFL). The comparative analysis of MFL with RMS in identification of muscle activation at different force levels (20%, 50%, and 80%) is presented in this chapter.

Chapter 7 reports on the application of fractal features (FD, MFL) in identification of finger & wrist actions using sEMG and measurement of the alertness level using Electroencephalogram (EEG).

Chapter 8 presents the conclusion of this work and discusses the main contributions of this research work.

Chapter 2

Literature Review

2.1 Introduction

This chapter provides an overall review of the various researches that have been conducted in the analysis of sEMG for measurement and properties of human muscle movements. The review in this section covers two major research areas:

- Use of sEMG signals in identification of subtle human movement, and
- Fractal theory based measurement analysis of sEMG

2.2 Review - Use of sEMG signals in identification of human movement

Surface Electromyogram (sEMG) is a myoelectric signal recorded from the surface of skeletal muscles and it indicates the functional state of muscle fibres (Duchêne and Goubel, 1993; Karlsson et al., 2000). It is a complex and non-stationary

signal with low signal to noise ratio (SNR). While the underlying mechanism of sEMG is complex with number of differing factors, it has been used in applications ranging from rehabilitation to sports medicine. Some of the applications include:

- Rehabilitation - Example: Assist system for the disabled (Nagata et al., 2005; Nagata and Magatani, 2004)
- Human computer control - Example: Control of pointing devices (Tsuji and Kaneko, 2000)
- Robotic and Prosthetic hand (Momen et al., 2007; Osamu Fukuda, 2004)
- Clinical applications - Example: assessment of muscle fatigue (Merletti et al., 2005) and low back pain (Rainoldi et al., 2005).

The ability to accurately interpret sEMG signals would enable and control the neuroelectrical interfaced systems. The design of these systems require the following two important factors to be considered as proposed by (Englehart and Hudgins, 2003):

1. Features of sEMG that can be related to different muscles and muscle activity, and
2. Classification paradigm of these features to identify these actions.

Numbers of researchers have identified a strong relationship between magnitude and spectral features of sEMG with the force of muscle contraction (Duchêne and Goubel, 1993). Various analogous measures such as

- root mean square (RMS) (Basmajian and De Luca, 1985),

- windowed integration and zero-crossing count (Basmajian and De Luca, 1985; Devaney, 1995),
- auto-regression (Barisi, 2007; Knox and Brooks, 1994), and
- wavelet coefficients (Kumar and Pah, 2000; Ren et al., 2006)

have been used to classify the signal against the desired movement and/or posture.

These features are easy to implement and are a good measure of the strength of muscle activity when there is a single active muscle that has high level of muscle activity. However these measures are not reliable when the muscle activity is very small and when there are multiple muscles that are simultaneously active. Alternate to the use of global parameters such as RMS, is to decompose sEMG and identify the action potentials (Karlsson et al., 2000; Kleine et al., 2007; Stashuk, 2001). The shortcomings in such techniques are that these require high level of manual supervision and are highly sensitive to the location of the electrodes. There are number of possible rehabilitation and defence applications of sEMG that are currently infeasible because there are no reliable features of sEMG that can be related to low-level of muscle contraction, without manual supervision.

The classification of these features has been achieved using a range of parametric and non-parametric techniques, ranging from Bayesian statistical classifiers, neural networks (Christodoulou and Pattichis, 1999; Kumar et al., 2001) and a predictive approach (Coatrieux et al., 1983). Some of the recent research work on classification of hand movements has been presented as follows:

- Nagata et al. presented a classification method of hand movements using 96 channels matrix-type (16x6) of multi-channel surface EMG (Nagata et al., 2005).

- Crawford et al. proposed the classification of electromyographic signals for robotic control using amplitude of five channels EMG as features and support vector machines as classifiers (Crawford et al., 2005).
- Englehert et al. used pattern recognition to process four channels of myoelectric signal (MES), with the task of discriminating multiple classes of limb movement (Englehart and Hudgins, 2003).
- Momen et al. used RMS of two channels EMG as features and segmented using fuzzy C-means clustering (Momen et al., 2007).

An example of the hand movement classification using surface electromyography is shown in Fig.2.1. The features used in these techniques are a good indicator of high level muscle activation. However at low- level of muscle contraction, these measures are not reliable in identifying the muscle activation from the background activity and requires a better classifier for separation of classes of movements. In order to determine the reliable measure of low-level muscle activity, there is need to extract a feature set from sEMG, that interprets the complex property of the muscle during subtle activity.

Most methods used to model and analyse sEMG are linear. However more complex activity such as sEMG recordings during small and complex maintained hand actions cannot be modelled by such linear techniques. With the need for identifying complex and subtle actions and gestures, nonlinear methods are emerging to characterize sEMG. The following three new approaches have been proposed in (Nussbaum, 2006) for characterisation of sEMG:

1. Methods that characterise the sEMG spectral distribution i.e., Logarithmic representation of sEMG spectrum

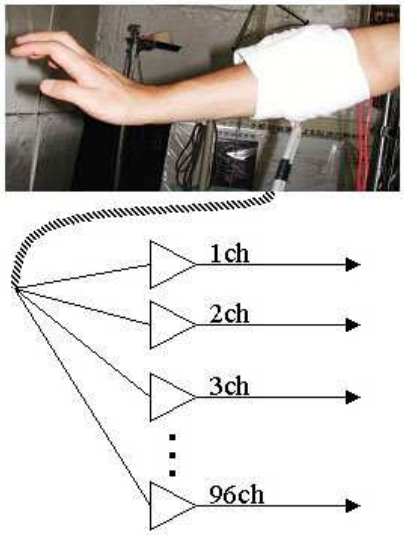

Figure 2.1: An example of hand movement analysis using multi-channel surface Electromyography [Source:(Nagata et al., 2005)]

2. Poisson representation of sEMG spectrum, and

3. Method that examines the 'complexity' of raw sEMG i.e., Fractal dimension of sEMG

Out of these approaches Fractal dimension (FD) of sEMG has been found sensitive to magnitude and change of force, because sEMG is self - similar over a range of scales (explained in *Chapter 4*) and the statistical properties of a part (structure of motor unit) are proportional to those of the whole (Gitter and Czerniecki, 1995; Gupta et al., 1997). These lieratures reviews lead to the study of fractal theory and use of fractal analysis of sEMG to determine the complex property of the muscle during subtle actvity.

2.3 Review - Fractal theory based analysis of sEMG

Fractals refer to objects or signal patterns that have fractional dimension. These objects exhibit self-similarity. This defines that the objects or patterns on any level of magnification will yield a structure that resembles the larger structure in complexity (Mandelbrot, 1977). The measured property of the fractal process is scale dependant and has self-similar variations in different time scales. Fractal dimension of a process measures its complexity, spatial extent or its space filling capacity and is related to shape and dimensionality of the process (Gitter and Czerniecki, 1995). The concept of fractal can be applied to physiological process that are self-similar over multiple scales in time and have broad band frequency spectrum. Fractals manifest a high degree of visual complexity (Gupta et al., 1997).

Biosignals such as sEMG are a result of the summation of identical motor units that travel through tissues and undergo spectral and magnitude compression. Burst within burst behaviour of sEMG in time has the property that patterns observed at one sampling rate are statistically similar to patterns observed at lower sampling rates. These nested patterns suggest that sEMG has self-similarity (Anmuth et al., 1994).

Researchers have studied fractal of sEMG to characterize normal and pathological signals (Acharya et al., 2005). To better represent the properties of sEMG signal, fractal dimension (FD) of sEMG has been proposed (Anmuth et al., 1994; Hu et al., 2005; Xu and Xiao, 1997). Recent studies of fractal analysis of sEMG is summarised as follows:

- Anmuth et al. determined that there is a change in fractal dimension of the surface EMG signal and is linearly related to the activation of the muscle measured as a fraction of maximum voluntary contraction. They also observed a linear relationship between the fractal dimension and the flexion-extension speeds and load (Anmuth et al., 1994).

- Gitter et al. determined that fractal dimension can be used to quantify the complexity of motor unit recruitment patterns. They also demonstrated that the fractal dimension of EMG signal is correlated with muscle force (Gitter and Czerniecki, 1995).

- Hu et al. distinguished two different patterns of FD of sEMG signals (Hu et al., 2005).

- Gupta et al. reported that the FD could be used to characterize the sEMG signal (Gupta et al., 1997).

FD represents the scale invariant, non-linear property of the source of the signal and is an index for describing the irregularity of a time series. FD is the property of the system or source of the signal (Mandelbrot, 1977) and in the case of sEMG, it is the property of the muscle. It should be a measure of the muscle complexity and not a measure of the level of muscle activity.

Research studies by (Gupta et al., 1997; Hu et al., 2005) have attributed the change in FD to the change in level of muscle contraction during high level muscle activity. Studies by (Basmajian and De Luca, 1985) have indicated that for low level of isometric muscle contraction, there is no change in the size of the muscle while there is measurable change in the muscle dimension during higher levels of muscle contraction and during non-isometric contraction.

Based on the above, this research work proposes to explain the small changes in the FD to the changes in muscle properties such as size and length due to the contraction and not to the changes in muscle force. Based on the above, this thesis proposes that for low-level of muscle contraction, FD would not change with change in the level of muscle contraction and that FD would be a measure of the size and complexity of the muscles.

2.4 Summary

This chapter has presented and described an overview of the recent work and the background on the use of sEMG in identification of human movement and the feature extraction methods for recognizing low-level muscle activation. This chapter has also presented recent studies on the use of fractal theory for analysis of sEMG. This literature review has discussed the strengths and limitations of the features used for identification of subtle muscle movements.
Based on the preliminary studies, this research proposes the following:

- Fractal dimension (FD) would not change with change in the level of muscle contraction and that FD would be a measure of the size and complexity of the muscles at low-level or subtle movements.
- Identification of new fractal measure of low-level muscle activity.
- Fractal features of sEMG for identifcation for complex and subtle gestures or movements using single channel sEMG.

This thesis identifies the fractal features of sEMG (*Chapter 5*), the performance analysis of these features and their comparison with RMS (*Chapter 6*),

and their applications (*Chapter 7*) based on the detailed study of sEMG and fractal theory (*Chapter 3 & Chapter 4*).

Chapter 3

Surface Electromyogram (sEMG)

3.1 Introduction

Surface electromyography (sEMG) is the recording of the muscle's electrical activity from the surface of the skin. In clinical application, sEMG is used for the diagnosis of neuro-muscular disorder and for rehabilitation. It is also used for device control applications where the signal is used for controlling devices such as prosthetic devices, robots, and human-machine interface.

The advantage of sEMG is due to its non-invasive recording technique and it provides a safe and easy recording method. The underlying mechanism of sEMG is very complex(Graupe and Cline, 1975) because there are number of factors such as neuron discharge rates, motor unit recruitment and the anatomy of the muscles and surrounding tissues that contribute to the recording. In this chapter basic concepts of generation of sEMG signals and its application will be described.

3.2 Generation of sEMG

SEMG signal is generated by the electrical activity of the muscle fibers active during a contraction. The signal sources located at the depolarized zones of the muscle fibers are separated from the recording electrodes by biological tissues, which act as spatial low-pass filters on the (spatial) potential distribution (Basmajian and De Luca, 1985). It is closely related to the muscle activity, muscle size and a measure of the functional state of muscle fibres (Huang and Chen, 1999). This section presents a brief explanation about the anatomy, physiology and the electrical properties of the muscle and the composition of sEMG.

3.2.1 Physiology of human muscular system

The physiology of the human muscular system has been explained as follows:

- **Structure of the muscle**

A muscle consists of a large number of muscle fibers that are grouped into several motor units. A motor unit is the basic level of the neuro motor system of the muscle. A motor unit (MU) consists of an α- motoneuron in the spinal cord and the muscle fibers it innervates. All the muscle fibers in a motor unit are controlled by a single motor neuron. The number of MUs per muscle in humans may range from about 100 for a small hand muscle to 1000 or more for large limb muscles (Moritani et al., 2005).

The number of muscle fiber per motor unit in a muscle is called the innervation ratio. The muscles of the face that execute a precise movement have the highest level of innervation ratio (3 muscle fibers per motor unit). The muscles that

produce a large amount of force have lower innervation ratio. Each muscle fiber in a motor unit is connected to each axon branch of the associated motor neuron at a point called *neuromuscular junction* (NMJ). The neuromuscular junction is located in a region in the middle of the muscle length called the innervation region. This is shown in Fig.3.1

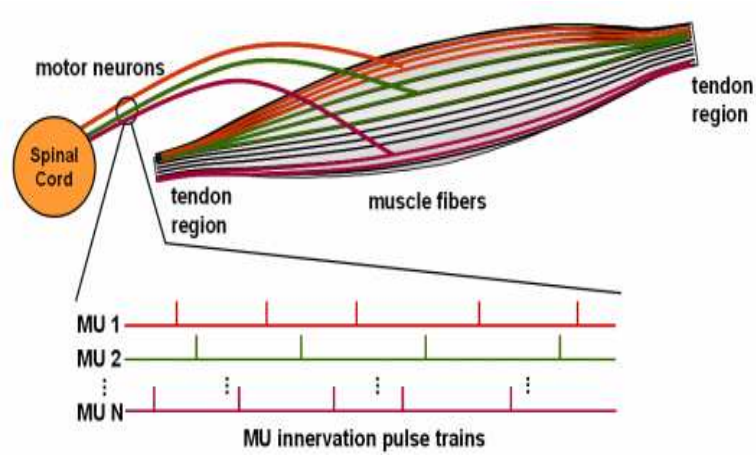

Figure 3.1: Muscle Structure and representation of Motor Unit [Source: DE-MUSE (Merletti, 2008)].

- **Muscle Contraction**

Muscle contraction is a result of the stimulations from motor neurons. Voluntary muscle contraction is used to move the body and can be finely controlled, such as movements of the finger or gross movements that of the biceps and triceps. There are three types of muscle contractions (Basmajian and De Luca, 1985):

1. *Isometric Contraction*

   In isometric contraction, the muscle is contracted while the length of the muscle is unchanged. These contractions are used in the postural control.

2. *Concentric contraction*

   Concentric contraction occurs when the length of the muscle shorten during the contraction. The amount of the available muscular energy in concentric contraction is less than the isometric contraction due to the energy loss related to the shortening of the muscle.

3. *Eccentric Contraction*

   Eccentric contraction occurs when the length of the muscle increases during the contraction. The concentric and eccentric contraction are also known as un-isometric contraction.

- **Recruitment Pattern**

The process of selecting which motor units to be involved in a muscle contraction is called the *recruitment* process. The current understanding of the motor unit recruitment pattern in a muscle is based on the *size principle*. This size principle was proposed by Henneman et al. (Henneman et al., 1965), who demonstrated that motor units are always recruited in order of increasing size of the α- motoneuron. For a small level of contraction, the motor units with small number of muscle fibers are recruited. As the contraction level increases, the larger motor units are involved in the contraction (Basmajian and De Luca, 1985; Cram et al., 1998). In an isotonic contraction which produces a constant force, the activation pattern switches from one motor unit to the other to avoid the fatigueness of a motor unit.

3.2.2 Motor Unit Action Potential (MUAP)

A motor neuron activates its motor unit by stimulating the motor unit's muscle fibers with the nerve action potential (AP) that travels along the axon towards the muscle fibers. The electric impulse that is propagated along the motoneuron arrives at its terminal and causes the emission of acetylcholine (ACh- a chemical substance) in the gap between the nerve terminal and the muscle fiber membrane, which excites the fiber membrane at this neuromuscular junction. In this case a potential gradient in a part of the fiber is generated (Farina et al., 2005). It creates the depolarisation zones on the muscle fibers that propagate away from the NMJ point in both directions towards the tendon (end point) of the muscle fiber.

The depolarisation occurs due to the sudden increase of the membrane permeability to sodium (Na+) (Cram et al., 1998) which results in a sudden influx of sodium into the muscle fiber. The process changes the resting potential of the fiber's cell to a level of electrical potential called *action potential*(AP). In general, the action potential can be characterized by a depolarization phase, a repolarization phase, and a hyperpolarizing long after potential.

The AP shape may change due to the conditions of the muscle and few stages of AP alteration can be distinguished during fatigue. In the beginning of fatigue, the AP spike width in space increases mainly because of the slowing of the repolarization phase. In this phase the rate of increase of the AP remains practically unchanged while the amplitude decreases slightly. The representation of the action potentials generated by the motor unit's fibers is shown in Fig.3.2.

The generation of the action potential creates an electric field in the suround-

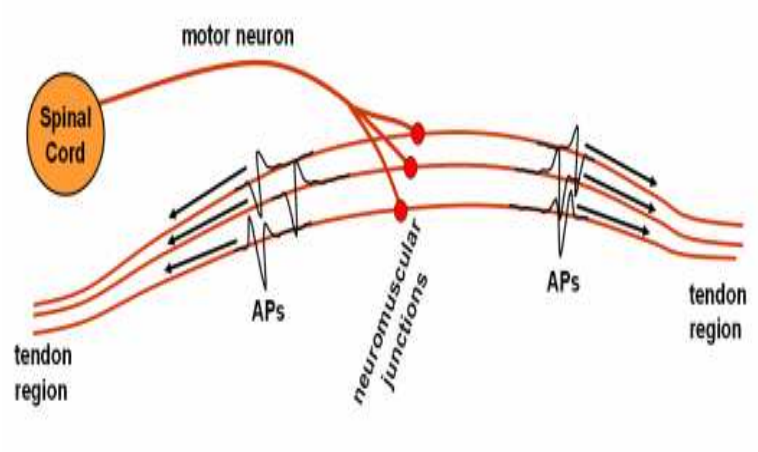

Figure 3.2: Representation of Single fiber action potentials (APs) [Source: DEMUSE (Merletti, 2008)].

ing space. Hence, the potential generated by motor unit can also be detected in locations relatively far from the source. The biological tissues separating sources and the detecting electrodes are referred to as *volume conductor* and their characteristics strongly affect the detected signal (Farina et al., 2005). The shape of the MUAP is affected by the geometrical arrangement of the muscle fibers, the electrode proximity and the properties of the body tissues between the muscle fibers and the recording site. MUAPs recorded with indwelling electrodes may have amplitude in the millivolt (mV) range, while the magnitude of the action potentials recorded with surface electrodes is of the order of microvolts (μV) (Basmajian and De Luca, 1985; Cram et al., 1998). Fig. 3.3 illustrates the superimposition of the MUAPs that results in the generation of sEMG.

Motor units must be activated repeatedly to sustain the force created by a muscle during a contraction. The frequency of the stimulation of a motor unit is called the *firing rate* of the motor unit. The firing rate determines the level of contraction and the type of muscle fibers. At the start of a contraction, a motor

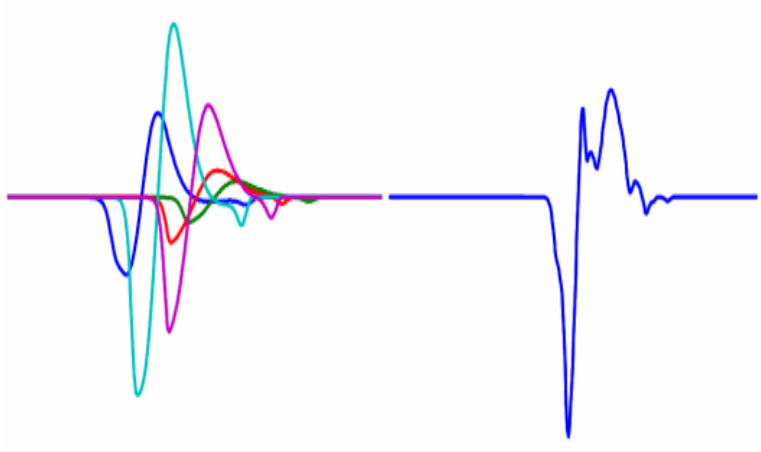

Figure 3.3: SEMG - the superimposition of all MUAPs generated in the surface of the skin [Source: DEMUSE (Merletti, 2008)].

unit is fired irregularly at a rate of about 5-7 Hz. As the level of contraction increases, the motor neuron increases the firing rate to higher frequency. As the firing rate reaches 10 Hz, the second motor unit is recruited into the contraction (Sandbrink and Culcea, 2002) while the firing rate of the first motor unit increases to a certain level according to the type of muscle fiber in the motor unit. In general, there are two categories of muscle fibers based on the speed of the firing rate. A slow twitch muscle fiber has a firing rate of about 10 to 20 Hz, while a fast twitch muscle fiber has 30 to 50 Hz firing rate.

3.3 Recording and detection of sEMG

SEMG is the recording of electrical potentials that appear on the surface of the skin due to the MUAP generated in the muscle fiber. Because of the size of recording electrodes, sEMG contains the summation of electrical activities from all of the active motor units in the location near the electrodes. The shape and

the amplitude of the surface action potential are also affected by the properties of the body tissue between the muscle fibers and the recording electrodes. The body tissue behaves as an imperfect insulator with low pass filter characteristic that tends to attenuate the higher frequency components of the signal. The recording

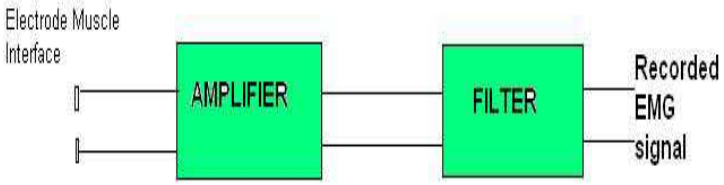

Figure 3.4: Block diagram of a basic sEMG recording system

system of sEMG consists of three basic block sets with electrodes, amplifier and filter as shown in the Fig.3.4. The surface electrodes are transducers that sense the current on the skin through its skin-electrode interface (Basmajian and De Luca, 1985). In order to record sEMG, the better understanding and design of the surface electrodes has to be studied. The advent of new processing techniques for extracting quantitative information from sEMG signal requires greater focus on the configuration of the electrode. The major points to consider are:

1. the signal to noise ratio of the detected signal,
2. the bandwidth of the signal,
3. the muscle sample size, and
4. the susceptibility to crosstalk.

- *Electrode configuration*

The electrodes can be configured either as a monopolar or as bipolar electrodes. SEMG recorded with a monopolar electrode contains the potentials that are recorded by the electrode with reference to the ground electrode. Bipolar electrodes record the potential difference between the two electrodes. The bipolar recording is a more suitable method due to its high noise reduction capabilities.

- *Location and orientation of the electrode*

  The electrode should be placed between a motor point and the tendon insertion or between two motor points, and along the longitudinal midline of the muscle. The longitudinal axis of the electrode (which passes through both detection surfaces) should be aligned parallel to the length of the muscle fibers.

The electrodes (Fig.3.5) used in this study are designed by DELSYS inc. This electrode configuration has some practical advantages:

1. It can be constructed so that it is sufficiently small and lightweight as to not be obtrusive to the subject.

2. The spacing of 1 cm between the detection surfaces is sufficiently large so as not to provide a prohibitive electrical shorting path when the skin sweats.

The magnitude of the recorded potentials is very small and have to be amplified with an amplifier that has high input impedance. An instrumentation amplifier with high input impedance and high common-mode rejection ratio (CMRR) is commonly used as the first stage in the recording instrumentation of sEMG. The instrumentation amplifier amplifies the differential signal while attenuating

the signal components that are common to both electrodes. This reduces external noise that is common to both electrodes, such as power line interference.

After the amplification, the signal is then filtered for the removal of unwanted frequency components of the signal. A band-pass filter at frequency of 20 to 500 Hz is commonly used in the sEMG recording instrument since most of the energy of sEMG signals reside in this frequency range (Cram et al., 1998). Beside the band-pass filter, a notch filter at 50 Hz is commonly applied to remove the power line interference at that frequency. In some cases, more filters are needed to eliminate other artefact such as movement artefact and ECG signal.

Figure 3.5: Surface Electrode from DELSYS inc. used for recording sEMG [Source: DELSYS (De Luca, 2006)]

For digital recording, the signal is sampled and coded with an analogue to digital converter (A/D) into streams of digital data. The sampling rate must be at least two times the highest frequency that appears in the signal to avoid the occurrence of aliasing. Anti-aliasing filter is also used to remove all frequency components above the half of sampling rate.

The advent of modern microelectronics has made possible the construction of amplifiers housed in integrated circuitry which have the required input impedance

and associated necessary characteristics. An example of such an electrode is presented in Fig.3.5. They each have two detection surfaces and associated electronic circuitry within their housing (De Luca, 2006).

3.3.1 Factors that influence sEMG

SEMG signal contains information related to muscle contraction and condition. Therefore, it is useful to analyse the signal to reveal the information without the need to intervene the muscle. The information immersed in sEMG signal is related to the following factors that influence the signal.

1. Level of Contraction

   The level of contraction affects the magnitude of the recorded sEMG (Cram et al., 1998). The magnitude of sEMG increases as the level of contraction increases as there is an increase in the number of motor units involved in the contraction.

2. Localised Muscle Fatigue

   Localised muscle fatigue can be observed from the shift of the median frequency of the signal towards the lower frequency and the increase in the signal's magnitude (Basmajian and De Luca, 1985; Cram et al., 1998; Kumar and Pah, 2000). This is due to the synchronisation of the stimulation of different motor units and the variation in the electrical properties of the muscle fibers.

3. The Thickness of Body Tissue

The body tissue tends to attenuate the high frequency component of the signal. The thicker the body tissue, the lower the frequency and amplitude of the signal are. SEMG signals recorded from facial muscle have a frequency of up to 500 Hz, while sEMG recorded from deep muscles have lower frequency range.

4. The Inter-electrode Distance

   The size and inter-electrode distance (IED) also have a known effect to the signal. If the distance between electrodes increases, the recording covers a wider area. As a result, the recorded signal consists of a larger number of action potentials, which lowers the frequency and increases the amplitude of the signal.

5. The Artefacts and Noises

   The properties of some of the noises and artefacts are predictable. The power-line interference appears sharply at 50 Hz, while the ECG artefacts appears at frequency up to 60 Hz (Cram et al., 1998). Although the frequency component of power-line and ECG components are well predicted, they are not easily removed due to the frequency overlapping between the artefacts and the sEMG spectrum.

6. Crosstalk muscle signals

   Crosstalk is the signal detected over a muscle but generated by another muscle close to the first one. The phenomenon is present exclusively in surface recordings, when the distance of the detection points from the sources may be relevant and similar for the different sources (Farina et al., 2005).

3.3.2 SEMG signal analysis techniques

SEMG signal is a time and force (and possibly other parameters) dependent signal whose amplitude varies in a random nature above and below the zero value. Thus, simple computation of average of the signal will not provide any useful information. Some of the measures of sEMG are explained below (De Luca, 2006):

- *Rectification*

  A simple method that is commonly used to overcome the above restriction is to rectify the signal before performing mode pertinent analysis.

- *Averages or Means of Rectified Signals*

  The equivalent operation to smoothing in a digital sense is averaging. By taking the average of randomly varying values of a signal, the larger fluctuations are removed, thus achieving the same results as the analog smoothing operation.

- *Integration*

  The most commonly used and abused data reduction procedure in electromyography is integration. It applies to a calculation that obtains the area under a signal or a curve. The units of this parameter are volt seconds (Vs). It is apparent that an observed sEMG signal with an average value of zero will also have a total area (integrated value) of zero. Therefore, the concept of integration may be applied only to the rectified value of sEMG signal.

- *Root-Mean-Square (RMS) Value*

Mathematical derivations of the time and force dependent parameters indicate that the RMS value provides a more rigorous measure of the information content of the signal because it measures the energy of the signal.

- *Zero Crossings and Turns Counting*

  This method consists of counting the number of times per unit time that the amplitude of the signal contains either a peak or crosses a zero value of the signal.

- *Frequency Domain Analysis*

  Analysis of sEMG signal in the frequency domain involves measurements and parameters that describe specific aspects of the frequency spectrum of the signal. Fast Fourier transform techniques are commonly available and are convenient for obtaining the power density spectrum of the signal.

These various measures are used to extract some meaningful information from sEMG for various applications. Currently, there are three common applications of sEMG (De Luca, 2006). They are:

- To determine the activation timing of the muscle; that is, when the excitation to the muscle begins and ends
- To estimate the force produced by the muscle.
- To obtain an index of the rate at which a muscle fatigues through the analysis of the frequency spectrum of the signal.

These information from sEMG are being used as a control input to activate or control various devices. This research study aims at using the informations of

sEMG from forearm to identify subtle finger and wrist movements, applications in human computer control and rehabilitation engineering. To determine these informations of sEMG from forearm, there is a need to study the anatomical and physiological properties of the forearm muscular system as described in the following section.

3.4 Anatomy and Physiology of forearm muscles

The forearm muscles are functionally divided into approximately equal groups: those causing wrist movements and those moving the fingers and thumb. In most cases, their fleshy portions contribute to the roundness of the proximal forearm and then they taper to long insertion tendons. Their insertions are securely anchored by strong ligaments called *flexor and extensor retinacula (retainers)*. Although many of the forearm muscles actually rise from the humerus (the humerus is a long bone in the arm or forelimb that runs from the shoulder to the elbow), their actions on the elbow are slight. Flexion and extension are the movements typically affected at both the wrist and finger joints. The anatomy of the forearm muscles explained here are referred from (Marieb, 1997).

The forearm muscles are subdivided into two main compartments:

- the anterior flexors and
- the posterior extensors

Each compartment has superficial and deep muscle layers. Eventhough the hand performs many different movements, it contains relatively few of the muscles

that control those movements. Most muscles that move the hand are located in the forearm and *operate* the fingers via their long tendons, like operating puppet by strings. This design makes the hand less bulky and enables to perform finer movements. The hand movements promoted by the forearm muscles are assisted and made more precise by small intrinsic muscles of hand. The physiological representation of the forearm muscles are presented in Fig.3.6 The locations and actions of the forearm muscles, which are responsible for wrist and finger flexions, are explained below (Marieb, 1997; Palastanga et al., 2006).

3.4.1 Brachioradialis

Brachioradialis is a muscle of the forearm that acts to flex the forearm at the elbow. It is also capable of both pronation and supination, depending on the position of the forearm. The brachioradialis is a stronger elbow flexor when the radioulnar joint (forearm) is in a mid position between supination and pronation. When the forearm is pronated, the brachioradialis is more active during elbow flexion. It is a synergist in forearm flexion and it acts to best advantage when the forearm is partially flexed and semi pronated. During rapid flexion and extension, it acts to prevent joint separation.

3.4.2 Flexor Carpi Radialis (FCR)

Flexor Carpi Radialis are a pair of muscles located in each of the lower-arms of the human body. In anatomy, flexor carpi radialis is a muscle of the human forearm that acts to flex and abduct the hand. It is a powerful flexor of wrist and synergist in elbow flexion.

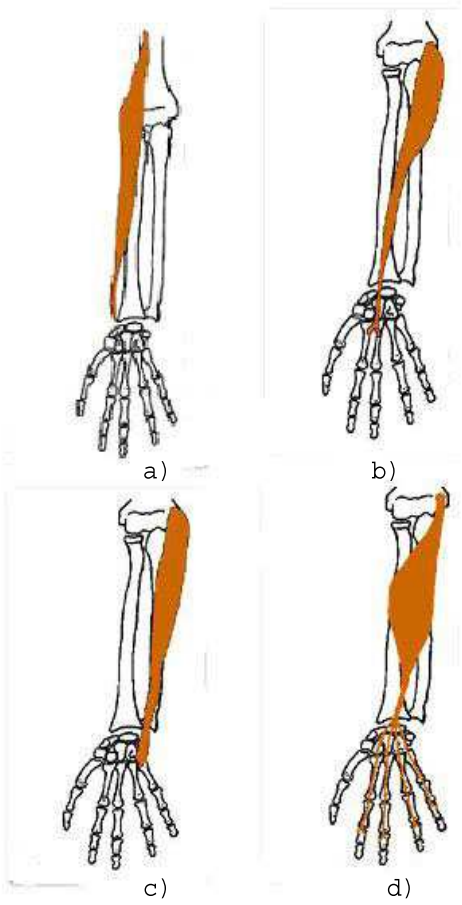

Figure 3.6: Physiological representation of the forearm muscles used in this research study. a. Brachioradialis b. Flexor Carpi Radialis c. Flexor Carpi Ulnaris d. Flexor Digitorum Superficialis [Source: (Palastanga et al., 2006)]

3.4.3 Flexor Carpi Ulnaris (FCU)

Flexor carpi ulnaris muscle (FCU) is a muscle of the human forearm that acts to flex and adduct the hand. It has its origins on the medial epicondyle of the humerus and the olecranon process of the ulna. It is a powerful wrist flexor and hand abductor working in concert with the extensor carpi ulnaris. It stabilizes the wrist during finger extension.

3.4.4 Flexor Digitorium Superficilialis (FDS)

Flexor digitorum superficialis (flexor digitorum sublimis) is an extrinsic flexor muscle of the fingers at the proximal interphalangeal joints. It is in the anterior compartment of the forearm. It is sometimes considered to be the deepest part of the superficial layer of this compartment and sometimes considered to be a distinct, *intermediate* layer of this compartment.

The primary function of FDS is flexion of the middle phalanges of the fingers at the proximal interphalangeal joints, however under continued action it also flexes the metacarpophalangeal joints and wrist joint. It flexes wrist and fingers 2-5 and it is an important finger flexor when speed and flexion against resistance are required.

3.5 Low-level muscle activation and sEMG

The muscle activation is at low-level when there is little movement in the corresponding muscle group. When the strength of muscle contraction is small, there is small overlap of the MUAP, for example, in simple wrist and finger flexion movements. This in result shows small changes in recorded sEMG, which in turn requires different measures in identifying these small changes.

The main criterion that influences these small changes in sEMG is the crosstalk between muscles. This is due to the volume conduction properties in combination with the source properties, and it is one of the most important source of error in interpreting sEMG signals. The problem is particularly relevant in cases where the timing of activation of different muscles is important, such as in movement analysis (Farina et al., 2005). The aim is to interpret these small changes in sEMG

during finger and wrist movements which has many applications in prosthesis and human computer interfaces.

3.6 Summary

In summary, this chapter provided an introduction to surface Electromyogram, its generation and detection. SEMG based interfaces generally involve signal acquisition from a number of differential electrodes, signal processing (feature extraction) and real-time pattern classification. Main studies in the domain of bioengineering have concentrated on the use of sEMG signals for control of prosthesis, rehabilitation and computer interfaces for users with motor disabilities.

Surface EMG is also used as a diagnostics tool for identifying neuromuscular diseases, assessing low back pain, kinesiology and disorders of motor control. Beyond medical applications, sEMG has been proposed for control of computer interfaces. It can also be used to sense isometric muscular activity where no movement is produced. This enables definition of a class of subtle motionless gestures to control interfaces without being noticed and without disrupting the surrounding environment (Costanza et al., 2005).

Chapter 4

Introduction to Fractal Theory

4.1 Introduction

In this chapter, an introduction to fractal theory and the recent progress in applying fractal analysis to human physiology is presented. Fractal geometry and chaos theory provide a new perspective to view the physiological signals in current scenario. Fractal geometry is a new language used to describe, model and analyze complex forms found in nature. Benoit Mandelbrot was largely responsible in defining fractals and he showed fractals can occur in many different places in both Mathematics and Science (Mandelbrot, 1977).

4.2 Definition of fractal

A fractal is a pattern that repeats itself on an increasingly smaller scale. Alternatively, it can be said that a fractal is a set of self-similar patterns. The word *fractal* was coined by Benoit Mandelbrot in the early 1970's. It was derived from

the Latin word fractus which aptly means *broken*, i.e., fragmented or irregular. Mandelbrot (Mandelbrot, 1977) observed that certain natural geometries, e.g., coastlines, terrain and clouds, exhibited a simplifying invariance under scale, i.e. their geometries possessed similarities that were invariant to changes in magnification or resolution. He discovered that this invariance to scale existed in a large variety of artificial and natural phenomena. This invariance to scale, i.e. *self-similarity*, is central to *Fractal Geometry*. A wide class of natural geometries appears to possess this underlying fractal character within a range of scale.

Fractals model complex physical processes and dynamical systems. The underlying principle of fractals is that a simple process that goes through infinitely many iterations becomes a very complex process. Fractals attempt to model the complex process by searching for the simple process underneath (Green, 1998). Fractal dimensions are used to measure the complexity of these objects. The important and famous two examples are Sierpinski triangle and the Koch curve, which are shown in Fig. 4.1 and Fig. 4.2 respectively (Mandelbrot, 1977).

4.2.1 Basic properties of fractal

Let 'F' represent a Fractal. The basic properties of 'F' are (Akujuobi and Baraniecki, 1992; Falconer, 1990):

(i) F has a fine structure i.e. detail on arbitrarily small scales.

(ii) F is too irregular to be described in traditional geometrical language, both locally and globally.

(iii) F has some self similarity, perhaps approximate or statistical.

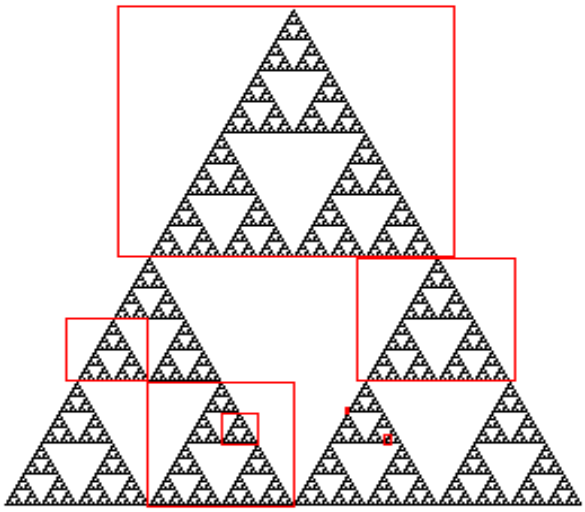

Figure 4.1: Sierpinski triangle [Source: (Green, 1998)]

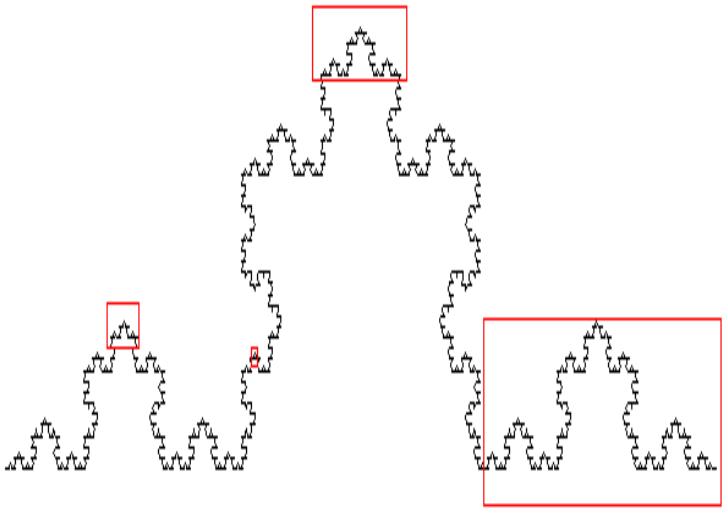

Figure 4.2: Koch curve [Source: (Green, 1998)]

(iv) Usually Fractal dimension of F is greater than its topological dimension.

The concept of a fractal is most often associated with geometrical objects satisfying the two important properties:

- self-similarity
- fractional dimensions

Mathematically, this property should hold on all scales but in the real world, there are necessarily lower and upper bounds over which such self-similar property applies. The second criterion for a fractal object is that it has a fractional dimension. This requirement distinguishes fractals from Euclidean objects, which have integer dimensions. As a simple example, a solid cube is self-similar since it can be divided into sub-units of 8 smaller solid cubes that resemble the large cube, and so on. However, the cube, despite its self-similarity, is not a fractal because it has a dimension = 3. (Bourke, 2007; Feder, 1988).

The concept of a fractal structure, which lacks a characteristic length scale, can be extended to the analysis of complex temporal processes. Although time series are usually plotted on a 2-dimensional surface, it actually involves two different physical variables. The important challenge is in detecting and quantifying self-similar scaling in complex time series (Bourke, 2007; Goldberger et al., 2000).

4.3 Self-similarity

An important defining property of a fractal is self-similarity, which refers to an infinite nesting of structure on all scales. In this section, the properties and definition of self-similarity are explained.

4.3.1 Definition and Properties

Self-similarity is a distinctive feature of most fractals. Self-similar processes are the ones in which a small portion of the process resembles a larger section when suitably magnified indicating scale invariance of the process. Self-similarity, in a strict sense, means that the statistical properties of a stochastic process do not change for all aggregation levels of the stochastic process. The stochastic process *looks the same* irrespective of any magnification of the process. The following will illustrate various types of self similarity as well as present some real world examples (Bassingthwaighte et al., 1994; Bourke, 2007; Feder, 1988; Iannaconne and Khokha, 1996).

- Exact self similarity

Exactly self-similar fractal objects are identical regardless of the scale or magnification at which they are viewed. Strict self-similarity refers to a characteristic of a form exhibited when a substructure resembles a superstructure in the same form. The well known *Koch snowflake* curve, a good example for this kind, has been created by starting with a single line segment and replacing each line segment by four other shapes on each iteration as shown in Fig. 4.3.

- Approximate self similarity

The more common type of self similarity is the approximate self-similarity. Approximate self-similar objects has recognisably similar object at different scales but are not exactly the same.

- Statistical self similarity

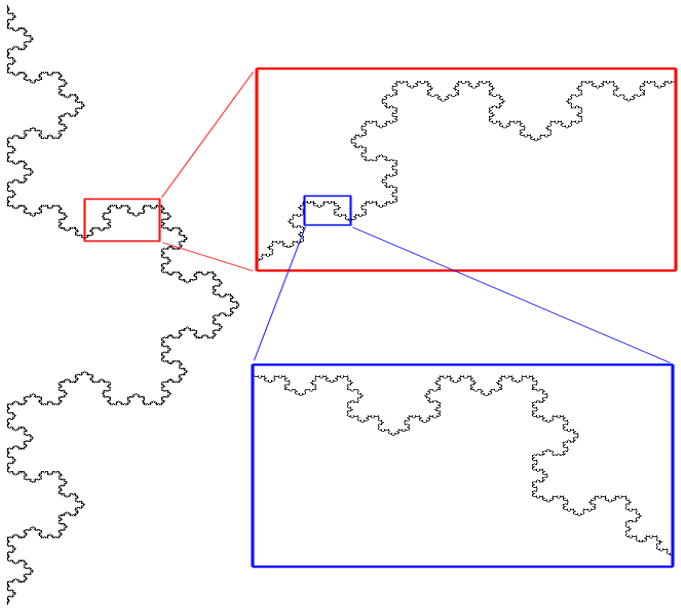

Figure 4.3: Example of exactly self-similar object [Source: (Bourke, 2007)]

The self-similar units of a time series signal sometimes cannot be visually observable but there may be numerical or statistical measures that are preserved across scales to determine the self-similar units. This is termed as *statistically self-similar*. Most physiological signals fall into the category of having statistically self-similar property. An example of statistical self-similar object is 1/f noise (Fig.4.4), where the units are statistically resemble across multiple zooming levels.

The self-similarity of a time series related process can be verified using the procedure (Kalden and Ibrahim, 2004) as follows:

- If $y(k)$ be a time series representing the process, then $y^{(m)}(k)$ is the aggregated process with non-overlapping blocks of size m such that:

$$y^{(m)}(k) = \frac{1}{m} \sum_{l=0}^{m-1} y(km - l)$$

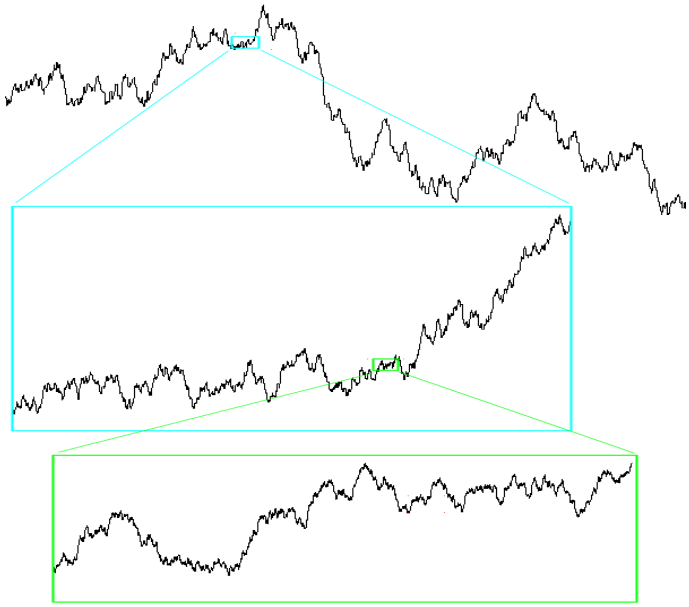

Figure 4.4: Example of statistical self-similar object [Source: (Bourke, 2007)]

- For the signal or process, $y(k)$ to be self-similar, the variance of the aggregated process decays slowly with m and this self-similarity is measurable by H , that is,

$$Var(y^{(m)}) \approx m^{-\beta}$$

with $0 < \beta < 1$ and

$$H = 1 - \beta/2$$

where H expresses the degree of self similarity; large values indicate stronger self-similarity.

- If $H\epsilon(0.5, 1)$ then the time aggregated series is long-range dependant (LRD).

It explains that the repeated occurrence of a particular pattern or a set of particular patterns creates a part and the whole time series. Fractal dimension can be applied to determine this statistical self- similarity i.e., the similarity between a part and the whole time series (Anmuth et al., 1994; Sarkar and Leong, 2003).

4.4 Fractal dimension (FD)

Fractal dimension of a process measures its complexity, spatial extent or its space filling capacity and is related to shape and dimensionality of the process. The concept of fractal can be applied to physiological processes that have self similar fluctuations over a multiple scale of time and have broad band frequency spectrum (Gupta et al., 1997).

4.4.1 Definition and Properties

There are many fractal dimensions reported in literature (Falconer, 1990; Feder, 1988; Lévy-Véhel and Lutton, 2006) including morphological (self-similarity, Hausdorff, mass), and entropy (gyration dimension, information, correlation, variance). The dimension is simply the exponent of the number of self-similar pieces with magnification factor N into which the figure may be broken.

Given a self-similar set S, the fractal dimension D of this set S defined as $ln(k)/ln(M)$ where k is the number of disjoint regions that the set can be divided into, and M is the magnification factor of the self-similarity transformation (Bassingthwaighte et al., 1994; Goldberger et al., 2000; Mandelbrot, 1977). This definition of the fractal dimension of a self-similar object is expressed as

$$\texttt{Fractal dimension} = \frac{\texttt{log(number of self-similar pieces)}}{\texttt{log(magnification factor)}} \tag{4.1}$$

A simple example of computation of fractal dimension of the Sierpinski triangle is illustrated below. Consider the Sierpinski triangle shown in the Fig. 4.1 consisting of 3 self-similar pieces, each with magnification factor 2. So the fractal dimension of this triangle as per the above expression (Eqn. 4.1) is

$$\texttt{Fractal dimension} = \frac{\texttt{log 3}}{\texttt{log 2}}$$

$$\texttt{= 1.58}$$

Hence the dimension of Sierpinski triangle is between 1 and 2. Fractal dimension is a measure of complexity of a self-similar structure and it measures how many points lie in a given set. A plane is *larger* than a line, while the dimension of Sierpinski triangle lies in between these two sets (Devaney, 1995).

The fractal properties of a time series signal can also be characterised by computation of fractal dimension. As explained in *Section 4.1,* the irregularity seen on different scales of time series is not visually distinguishable, an observation that can be confirmed by statistical analysis (Kobayashi and Musha, 1982; Peng et al., 1999). The roughness of the time series signals like biosignals, possesses a self-similar or scale-invariant property and their complexity can be analysed using fractal dimension.

4.5 Summary

The fractal theory was studied for its use in the analysis of physiological time series for its complexity. The nonlinearity of physiological systems may have relevance for modelling complicated surface electromyogram (sEMG), for example, low-level movements in which interactions and *cross-talk* occur over a wide range of temporal and spatial scales. A fundamental methodologic principle underlying these interpretations is important for analyzing continuously sampled variations in physiological output, such as muscle activity. Dynamical analysis demonstrates that there is often hidden information in physiological time series and that certain fluctuations previously considered *noise* actually represent important information (Goldberger et al., 2000; Ivanov et al., 1998; Peng et al., 1999). This research proposes the use of fractal theory in sEMG for identification of low-level muscle contraction as explained in the next chapter.

Chapter 5

Fractal anlaysis of sEMG

5.1 Introduction

Rehabilitation process, clinical diagnosis and basic investigations are critically dependent on the ability to record and analyze physiological signals like ECG, EEG and EMG. However, the traditional analyses of these signals have not kept pace with major advances in technology that allow for recording and storage of massive datasets of continuously fluctuating signals. Although these typically complex signals have recently been shown to represent processes that are non-linear, non-stationary, and non-equilibrium in nature, the methods used to analyze these data are often assume linearity, stationarity, and equilibrium-like conditions. Such conventional techniques include analysis of means, standard deviations and other features of histograms, along with classical power spectrum analysis (Goldberger et al., 2000).

Recent findings (Chen and Wang, 2000; Kleine et al., 2007; Lowery and O'Malley, 2003) show that sEMG signals may contain hidden information that

is not extractable with conventional methods of analysis. Such hidden information promises to be of clinical value as well as to relate to basic mechanisms of muscle property and activity function. Fractal theory based analysis is one of the most promising new approaches for extracting such hidden information from physiological time series signal like sEMG, which can provide information regarding the characteristic temporal scales and the adaptability of muscle activity response (Bassingthwaighte et al., 1994; Bourke, 2007; Feder, 1988; Goldberger et al., 2000).

This chapter presents a novel method on extracting information from sEMG using fractal based analysis. The framework of this method is to determine the fractal features of sEMG and their relation to the low level muscle activity pattern. Identification of subtle movements requires more information, related to subtle changes in the muscle activation from sEMG signal. It is very difficult for the traditional methods to extract information from the small changes in sEMG. As these sudden transients of sEMG is due to the properties of muscle and its activity pattern, the features relating to these properties has to be identified.

This study identifies the two important features including a new fractal feature, based on the important properties of muscle activity pattern:

- Fractal dimension (FD) - a measure of complexity of different muscles
- Maximum Fractal Length (MFL) - a measure of muscle activation

Section 5.2 presents a preliminary analysis on self-similarity property of sEMG, a basis of fractal analysis. *Section 5.3* describes the Fractal dimension of sEMG as a measure and its relation to the complexity of muscle. Maximum Fractal Length, a novel feature as a measure of low-level muscle activation, is discussed

in *Section 5.4*. Finally, *Section 5.5* summarizes the properties of proposed fractal features of sEMG that is used for recognition of low-level muscle activity pattern.

5.2 Self-similarity of sEMG

In complex bio signals like sEMG, there exists self similarity phenomenon, in which there is a small structure (motor unit) that statistically resembles the larger structure. The source of sEMG is a set of similar action potentials originating from different locations in the muscles. Because of the selfsimilarity of the action potentials that are the source of the sEMG recordings over a range of scales, sEMG has fractals properties.

Preliminary analysis was performed to establish the suitability of the use of fractal analysis of sEMG recordings. The recording of sEMG while performing simple contraction was conducted to test the presence of self-similarity. To determine the self-similarity in the recorded muscle activity (sEMG), the procedure explained in *Section 4.2* was followed :

- A new time series $y^{(m)}(k)$ of the aggregated sEMG signal over m was generated from the recorded sEMG signal.

$$y^{(m)}(k) = \frac{1}{m} \sum_{l=0}^{m-1} y(km - l)$$

- The natural log of variance between the original and the aggregated series was plotted against the natural log of m. This is shown in the Fig.5.1.

- From the Fig.5.1, it is observed that the variance decays slowly with m with

$$\beta = 0.9573 < 1 \ .$$

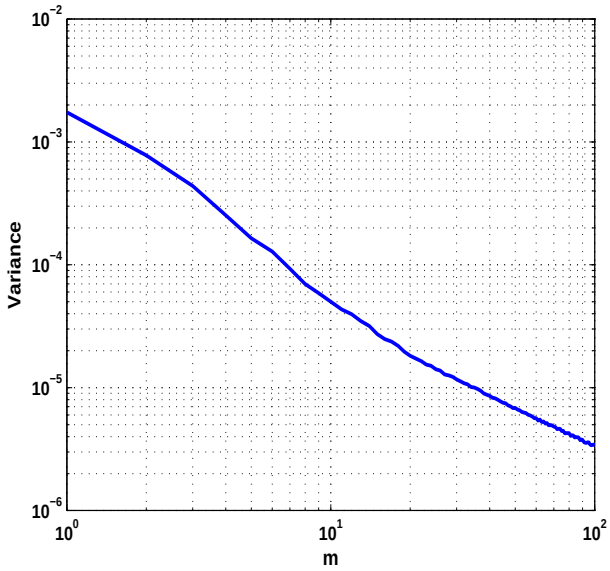

Figure 5.1: Logarithmic plot of the variance and the scale m for a sample sEMG recording to determine the self-similarity property

- From this β value and the plot in Fig.5.1, the self-similarity index of recorded sEMG signal was computed with

$$H = 0.5213$$

Based on the value of β being less than 1, it is confirmed that the signal has self-similarity and is long-range dependant (LRD). This confirms the use of fractal dimension to determine this self-similar property of sEMG, while determining the muscle properties and muscle activation.

5.3 Method to determine Fractal dimension

Fractal dimension (FD) analysis is frequently used in physiological signal processing like sEMG, EEG, ECG (Durgam et al., 1997; Gupta et al., 1997; Peng

et al., 1999). Applications of FD in these physiological signals include two types of approaches (Esteller et al., 2001):

- *Signals in the time domain*

  The former approaches estimate the FD directly in the time domain or original waveform domain, where the waveform or original signal is considered a geometric figure and,

- *Signals in the phase space domain*

  Phase space approaches estimate the FD of an attractor in statespace domain.

Calculating the FD of waveforms is useful for transient detection, with the additional advantage of fast computation. It consists of estimating the dimension of a time-varying signal directly in the time domain, which allows significant reduction in program run-time (Esteller et al., 2001). The FD of sEMG is calculated to determine the transients in sEMG, that is related to the overall complexity of the muscle properties. Three of the most following prominent methods for computing the FD of a waveform (Higuchi, 1988; Katz, 1988; Petrosian, 1995) have been applied to the analysis of signals, and a variety of engineering systems.

- Higuchi's Algorithm
- Katz's Algorithm
- Petrosian's Algorithm

Study by (Esteller et al., 2001) have shown that *Higuchi's* algorithm provides the most accurate estimates of the FD. *Katz's* method was found to be less linear

and its calculated FDs were exponentially related to the known FDs, whereas *Petrosian's* algorithm was found to be relatively linear and demonstrated the least dynamic range for the estimated FD. Based on this, *Higuchi's* algorithm was considered for the computation of FD of sEMG in this study.

5.3.1 Algorithm

Fractal dimension was calculated using the procedure reported by Higuchi (Higuchi, 1988) for non-periodic and irregular time series. This procedure yields a more accurate estimation of fractal dimension (Esteller et al., 2001). This reported technique can give stable indices and time scale, corresponding to the characteristic frequency even for a small number of data.

Procedure:

- Consider a finite set of time series observations taken at a regular interval:

$$X(1), X(2), X(3), ..., X(N)$$

- From the given time series, construct a new time series, X_k^m, defined as follows:

$$X(m), X(m+k), X(m+2k), ...X(m+\left[\tfrac{N-m}{k}\right].k) \;\&\; (m = 1, 2, ..., k)$$

  Where $[\ ]$ denotes the Gauss' notation and both k and m are integers. m = initial time; k = interval time

- Defining the length of the curve, X_k^m, as follows:

$$L_m(k) = \frac{\left(\sum_{i=1}^{\left[\frac{N-m}{k}\right]} |X(m+ik) - X(m+(i-1).k)|\right) \frac{N-1}{\left[\frac{N-m}{k}\right].k}}{k} \tag{5.1}$$

The term, $N-1/[(N-m)/k].k$, represents the normalization factor for the curve length of subset time series.

- The length of the curve for the time interval $\langle k, (L(k))\rangle$, is defined as the average value over k sets of $L_m(k)$. If $\langle L(k)\rangle \ \alpha \ k^D$, then the curve is fractal with the dimension D for a statistically self-similar curve.

The straight line is fitted to the points by the least-square method to determine the slope. This slope represents the fractal dimension.

5.3.2 Relation of FD to sEMG

Fractal dimension of sEMG has been found sensitive to magnitude and rate of muscle force generated. Fractal dimension is introduced as the index for describing the irregularity of a time series in place of the power law index. Gitter et al. (Gitter and Czerniecki, 1995) demonstrated that the fractal characteristics of EMG signal with a dimension is highly correlated with muscle force. Gupta et al. (Gupta et al., 1997) reported that the fractal dimension can be used to characterize the sEMG signal. Hu et al. (Hu et al., 2005) distinguished two different patterns of fractal dimensions of sEMG signals. These studies demonstrated that fractal information of sEMG is useful for characterizing the signal and identifying properties of the signal.

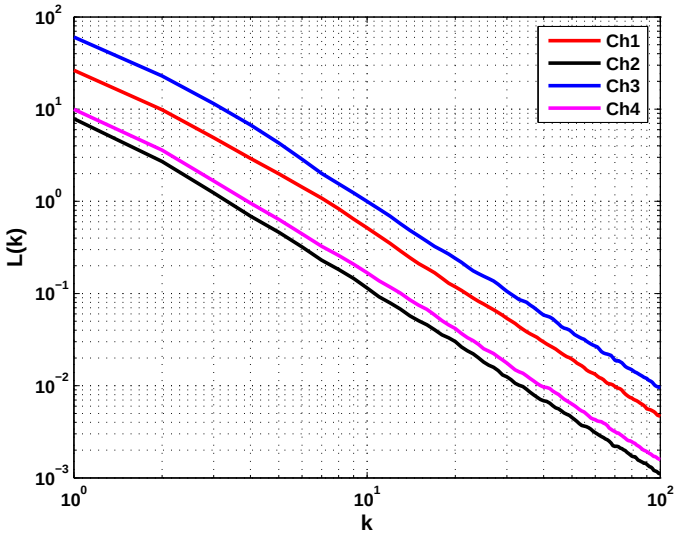

(a)

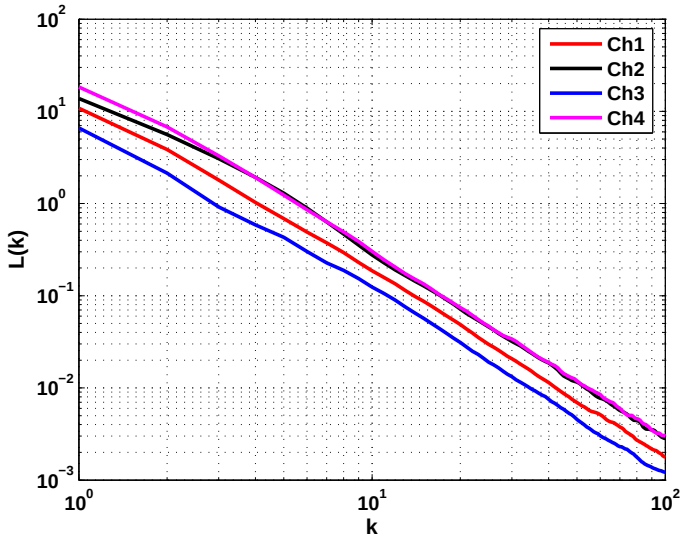

(b)

Figure 5.2: Logarithmic plot of the curve length $\langle L(k) \rangle$ and scale k for the four channel recorded sEMG signal during two different simple flexions (a) Wrist flexion and (b) all fingers flexion

Researchers have studied fractal dimension to characterize normal and pathological signals (Acharya et al., 2005). Anmuth et al.(Anmuth et al., 1994) determined that there was a small change of the fractal dimension of the sEMG signal and this was linearly related to the activation of the muscle measured as a fraction of maximum voluntary contraction. They also observed a linear relationship between the fractal dimension and the flexion - extension speeds and load. FD of a process measures its complexity, spatial extent or its space filling capacity and is related to shape and dimensionality of the process (Gitter and Czerniecki, 1995; Mandelbrot, 1977).

The most important inherent properties of muscle include muscle dimensions and complexity. These properties may change with the change in shape and contraction of the muscle and presence of other simultaneously active muscles. While high level of contraction or muscle stretch would also have an impact on FD (Gupta et al., 1997), there would not be significant variations of FD with small changes of muscle contraction. Studies by Basmajian and De Luca (Basmajian and De Luca, 1985), have indicated that for low level of isometric muscle contraction, there is no change in the size of the muscle.

During low level contraction the underlying self-similar process (muscle) remains unchanged, but there is a small change in the density of MUAP. It is expected that the FD will remain unchanged even though the force of muscle contraction would change. FD will be indicative of the process that in this case is the muscle itself. These facts lead to the hypothesis that: *More complex the muscle structure, higher would be the magnitude of FD.* The rate of increase in the average length of signal, calculated using the algorithm, with decreasing scale will be greater for more complex and bigger muscles which would have a larger

number of active motor units. This is due to the fact that MUAP originating from superficial muscles have higher frequency and magnitude compared to the MUAP originating from deeper muscles (Holobar and Zazula, 2003; Huiskamp et al., 1995; Kleine et al., 2007).

In order to determine the significance of FD and its relation to sEMG, preliminary analysis was conducted by using recorded sEMG while performing low-level wrist and fingers flexion. This analysis show that FD of sEMG resulting from deeper muscles is significantly less than from superficial muscles and signal from very distant muscles do not have fractal properties. Fig.5.2 shows the computation of FD of sEMG recorded from each forearm muscle. From this plot, it is observed that the FD i.e., slope of the line, for different channels does not vary much. The reason for this no observable changes in FD, is attributable to the same length and complexity of the forearm muscles, at low-level contraction. While high level of contraction or muscle stretch would also have an impact on FD (Gupta et al., 1997), there would not be significant variations of FD with small changes of muscle contraction.

Based on the above facts, it is proposed that for low-level of muscle contraction, FD would not change for small changes in muscle contraction and that FD would be a measure of the size and complexity of the muscles. Hence FD is a very useful feature of sEMG to measure the overall fractal property of the signal. However, the functionality of muscle contraction is dependent on the strength of contraction as well as the complexity of the different muscles. There is a need for identifying another feature of fractals that would provide more information of sEMG for determining the resultant function being performed.

5.4 Determining a novel feature - Maximum fractal length

To identify small actions, it is important to be able to determine the subtle changes in the sEMG. While FD is a measure of complexity of the muscle, the average length of the signal at corresponding scales from the fractal dimension algorithm is a measure of the small changes in the muscle activation.

When the strength of the muscle contraction is very small, there is small or no overlap of the MUAP. Each MUAP contributes to a singularity in the recording and in turn the length of the signal. The addition of singularity will lead to the small change in the length of the signal. This small change can be identified from the fractal length at lower scales, where the length is maximal for each contraction. Hence it is proposed that the average fractal length $\langle L(k) \rangle$ of the signal (over unit time) measured at the smallest scale from the fractal dimension algorithm to be used as a measure for low level muscle contraction. This has been identified as a novel feature and referred to as *Maximum Fractal Length (MFL)*.

The changes in low-level muscle contraction leads to the change in length of the signal at smallest scale measured from the log-log plot. From Fig.5.5 and Fig.5.6, it is observed that the lengths at higher scales were similar for different channels for the same flexion. Based on this, higher scales were not considered for this study.

The Maximum Fractal length is determined from the fractal dimension algorithm explained in *Section 5.3* and it is defined as

$$\texttt{MFL} = \langle L(k) \rangle_{\texttt{at smallest scale}}$$

where $\langle L(k) \rangle$ is determined from Eqn.5.1.

The computation of MFL of sEMG is shown in the Fig.5.3. The use of MFL as a measure of changes in sEMG during low-level contraction and its reliability over the background noise, has been explained in the next section.

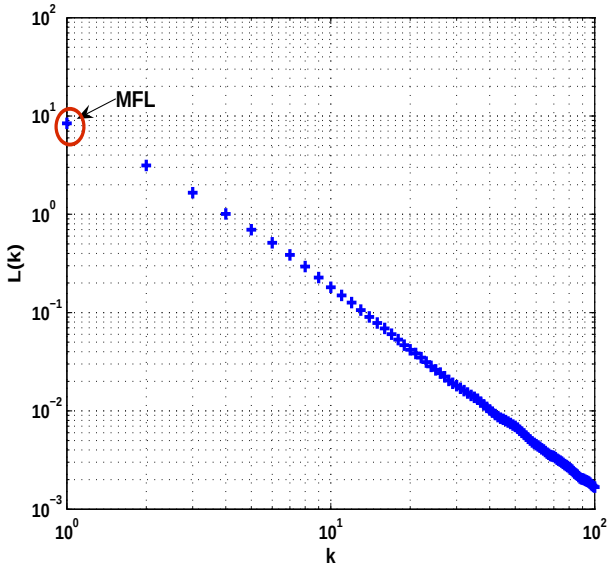

Figure 5.3: Computation of MFL from the fractal dimension algorithm

5.4.1 Relation of MFL to sEMG

A preliminary analysis was peformed to determine the relation of MFL to the properties of sEMG. For this analysis, sEMG from four channels (sensors placed on surface of different muscles) in forearm while performing subtle finger and wrist flexions were considered. MFL was computed using the procedure explained in *Section 5.4* and as shown in the Fig.5.4.

This MFL represents the level of muscle activity for the particular gestures. The logarithmic plot of the modified sEMG signal for each of the four channels

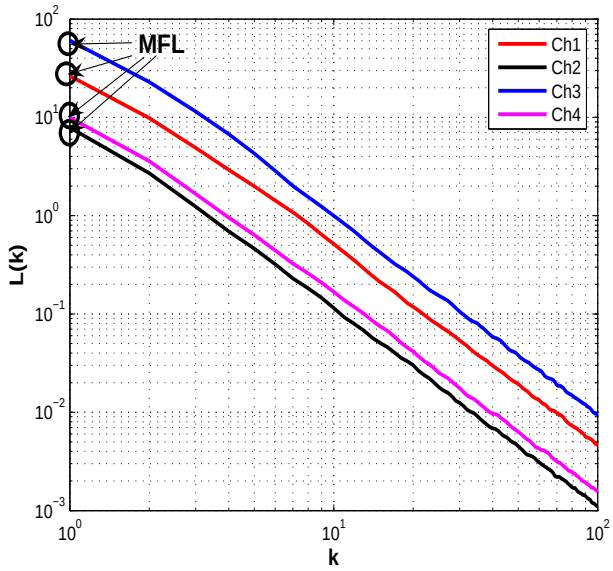

Figure 5.4: MFL of four channel sEMG data computed from the fractal dimension algorithm

for all forearm subtle gestures were plotted. Each individual plot contains the curve for four channels for the each of the hand gesture. This is shown in Fig.5.5 and Fig.5.6. This gives different pattern of the four channels for the different gestures.

From the analysis and the plot, there are some common observations:

- For wrist flexion gesture, Channel 2 has higher MFL i.e., level of muscle activity (refer Fig.5.5)
- For wrist flexion gesture towards little finger in horizontal plane, Channel 3 has higher MFL which relates to the muscle anatomy (Palastanga et al., 2006)
- While for fingers flexion gestures, Channel 4 has higher MFL at lower scales and as the line decays it overlaps with Channel 2 and Channel 1 at higher

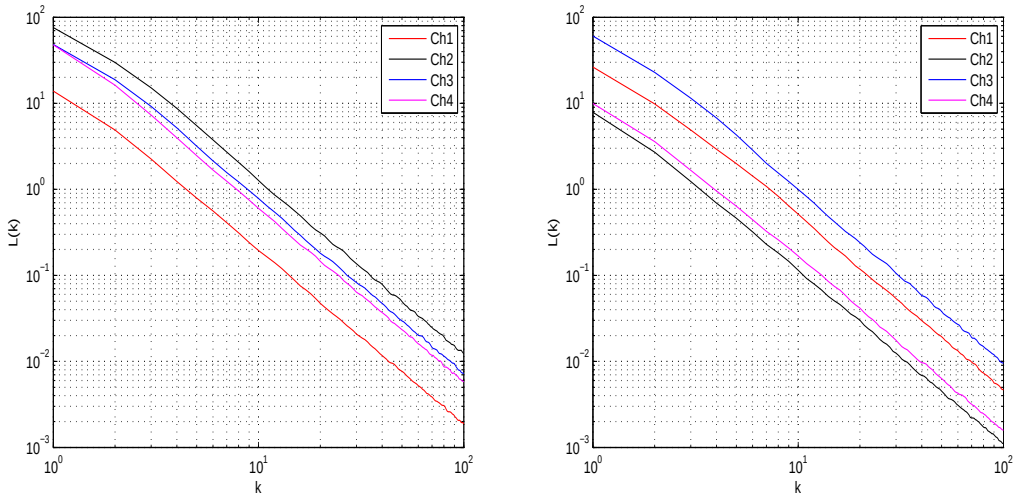

(a) (b)

Figure 5.5: Example of Logarithmic plot of the curve length $\langle L(k) \rangle$ and scale k for the four channel recorded sEMG signal during two different Wrist flexions

scales (refer Fig.5.6). This may be due to the overlap of recruitment of motor units for this particular gestures.

The results show that MFL value changes with respect to the small changes in the muscle actvity eventhough the slopes of the channels corresponding to FD remains unchanged. This suggest that MFL is a measure of muscle actvity even when the level of muscle activity is very low and it varies with respect to the changes in the sEMG.

5.5 Summary

Fractal analysis of sEMG has been presented in this chapter to identify and relate to the properties of sEMG during sustained low-level muscle contraction. Number of researchers have studied fractal properties of sEMG, but the earlier

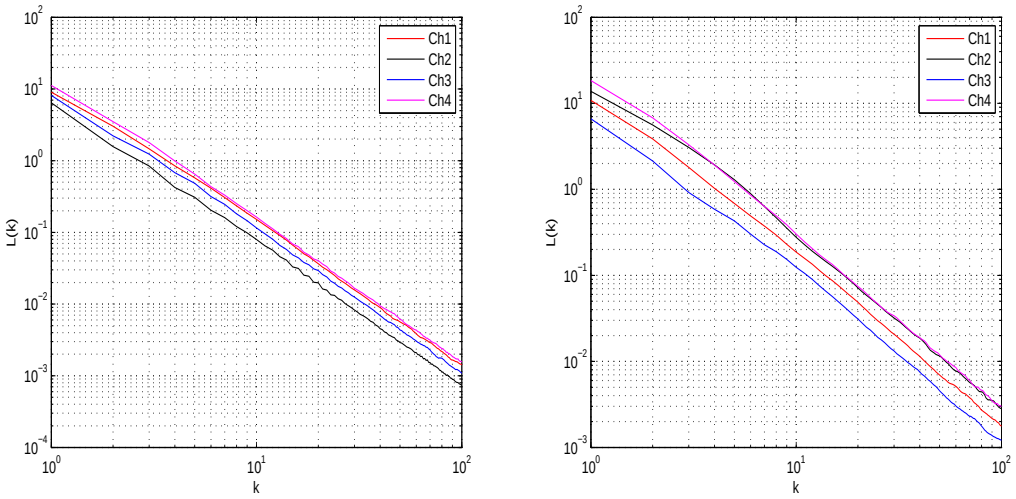

Figure 5.6: Example of Logarithmic plot of the curve length, $\langle L(k) \rangle$ and scale k for the four channel recorded sEMG signal during two different fingers flexion

studies have linked the fractal dimension (FD) to the strength of muscle contraction (Gitter and Czerniecki, 1995; Gupta et al., 1997; Hu et al., 2005). This preliminary study reports that FD does not vary for small changes in isometric muscle contraction. A new fractal based features of sEMG has been identified which is closely related to the strength of the muscle activation even when the strength of muscle contraction is very small. It is based on the fractal length of the signal at the lowest scale and is termed as Maximum Fractal Length (MFL). It is observed that there is a close relationship between the muscle activity and MFL - *MFL increases with increase in the muscle activity.* The results demonstrate that MFL is suitable for measuring force of muscle contraction while at low levels of muscle contraction.

For small variations in muscle contraction, there is only very small change in the value of FD while there is a significant change in MFL. The preliminary

experiments indicate the use of FD and MFL for complex action recognition, especially when the level of contraction is small, such as during sustained isometric forearm contraction. The performance evaluation of these fractal features, FD and MFL of sEMG are described in the next chapter.

Chapter 6

Analysis of fractal features - FD and MFL - of sEMG

6.1 Introduction

This chapter reports on the experimental analysis of fractal features of sEMG. This analysis was performed to determine

- FD - as a measure of muscle property, and
- MFL - as a measure of muscle activation

The experiments were conducted to evaluate the performance of FD & MFL as a measure of muscle properties and low-level muscle activity. The performance of FD and MFL were examined using two different experimental analysis as explained in below sections:

- *Section 6.2* reports on the first part of the experiments that investigated the relationship between FD and the muscle properties. The statistical

analysis was done to evaluate the performance of FD with the contraction of different size and length of muscles at different levels of force (20%, 50% and 80%).

- *Section 6.3* presents the second part of the experiments that evaluated the performance of MFL as a new measure of low-level muscle activity. The statistical comparison between the MFL and RMS was done to evaluate the performance of these measures for identifying muscle activity at different levels of force (20%, 50% and 80%).

6.2 Experimental Analysis of performance of FD as a measure of muscle properties

The first part of the experiment was conducted to validate the hypothesis that FD is a measure of muscle property and is not a measure of muscle activation when there is low-level muscle actvity. The experimental analysis was also performed to identify the relationship between FD and the muscle properties and the following were observed:

- larger the muscle higher the fractal dimension(FD)
- very small and insignificant variation in FD when there is low-level muscle activation for the same length of muscle.

The experimental setup and protocol is explained in the following section.

6.2.1 Experimental setup

6.2.1.1 Subjects

Seven healthy subjects (Six male and one female) volunteered to participate in this study. Mean age was 26.6 ± 2.05 years with mean weight = 70.6 ± 6.56 kg and mean height = 170.6 ± 7.42 cm. The participants exclusion criterion was; (i) no history of myo or neuro-pathology, and (ii) no evident of abnormal motion restriction. Experiments were conducted after receiving approval from RMIT University Ethics Committee for Human Experiments. Each participant was given an oral and written summary of the experimental protocol and the purpose of the study and was asked to sign a consent form prior to participation.

6.2.1.2 Muscles Studied

To determine the relationship between the FD and the muscle properties, different muscle groups with varied complexity was studied anatomically. For this study, four set of muscles were examined (Table 6.1) (Chang et al., 1999; Marieb, 1997; Palastanga et al., 2006). Quadriceps, Biceps and Flexor Digitorium Superficialis (FDS) muscles maintained isometric contraction against a fixed surface while Zygomaticus muscle maintained visually isometric contraction. The description of these muscle groups are as follows:

- Zygomaticus Muscle(Facial)
  - Muscle pair extending diagonally from corner of mouth to cheekbone
  - Raises lateral corners of mouth upward (smiling muscle)
- Biceps brachi

  - Two-headed fusiform muscle; tendon of long head helps stabilize shoulder joint
  - Flexes elbow joint and supinates forearm

- Quadriceps Rectus femoris
  - Superficial muscle of anterior thigh; runs straight down thigh; longest head and only muscle of group to cross hip joint
  - Extends knee and flexes thigh at hip

- Forearm Muscles - FDS
  - The flexor/pronator group and extensor/supinator group occupies the anterior and the posterior compartment of the forearm respectively
  - These muscles are responsible for movement of the forearm, wrist, and digits

Table 6.1: Different types of muscle and their size and complexity used in this study

Name of muscle	Size and complexity
Quadriceps femoris	Largest in length and most powerful muscle in the body
Biceps brachii	Medium in length and elbow flexor
Flexor digitorium superficialis	Smaller than Biceps brachii and more complex with more closely located muscles
Zygomaticus	Small and complex muscle

6.2.1.3 SEMG recording and processing

Surface Electromyographic (sEMG) recordings were obtained using a proprietary surface EMG acquisition system by DELSYS (Boston, MA, USA)[Fig.6.1]. The parallel-bar EMG sensor (refer Fig.6.1) was used for sEMG recording. Each channel is a pair of differential electrodes with a fixed inter-electrode distance of 10mm and a gain of 1000. sEMG signal was bandpass filtered with cut-off frequency between 20-450Hz. Prior to placing the electrodes, skin of the participant was prepared by shaving (if required) and exfoliation to remove dead skin. Skin was cleaned with 70% v/v alcohol swab to remove any oil or dust from the skin surface. The skin impedance between the two electrodes was measured and in all cases was less than 60 $K\Omega$. Standard isometric manual muscle testing was performed to verify electrode placement (Basmajian and De Luca, 1985; Fridlund and Cacioppo, 1986; Hermens et al., 2000).

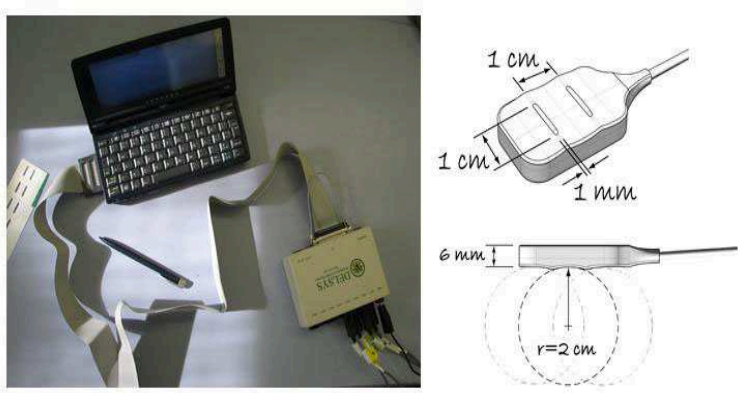

Figure 6.1: DELSYS surface EMG acquisition system and the parallel-bar EMG sensor

Along with sEMG recording, the force of each muscle contraction was measured using *FlexiForce* sensor in order to measure and maintain the different

Maximum voluntary contractions (MVC). *FlexiForce A201* (Tekscan, Boston, MA, USA)(refer Fig. 6.2) force sensor is an ultra-thin, flexible force sensor that can be fixed to measure the force of contraction. The force sensors are constructed of two layers of substrate (polyester/polyimide) film. On each layer, a conductive material (silver) is applied, followed by a layer of pressure-sensitive ink. Adhesive is then used to laminate the two layers of substrate together to form the force sensor. The active sensing area is defined by the silver circle on top of the pressure-sensitive ink. Silver extends from the sensing area to the connectors at the other end of the sensor, forming the conductive leads. A201 sensors are terminated with male square pins, allowing them to be easily incorporated into a circuit. The two outer pins of the connector are active and the center pin is inactive.

FlexiForce single element force sensor acts as a force sensing resistor in an electrical circuit. When the force sensor is unloaded, its resistance is very high. When a force is applied to the sensor, this resistance decreases. The resistance can be read by connecting a multimeter to the outer two pins, then applying a force to the sensing area.

One way to integrate the *FlexiForce A201* force sensor into an application is to incorporate it into a force-to-voltage circuit. A means of calibration must then be established to convert the output into the appropriate engineering units. The design of the circuit is shown in the Fig. 6.2. Depending on the setup, an adjustment could then be done to increase or decrease the sensitivity of the force sensor.

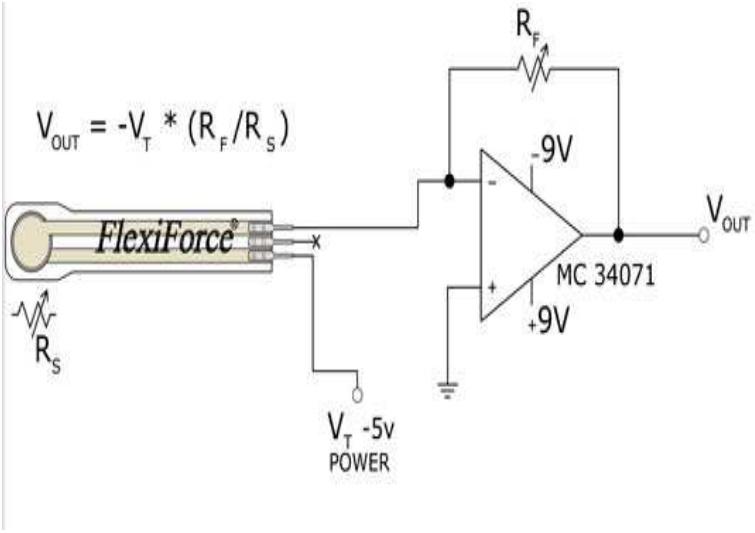

Figure 6.2: Force-to-Voltage circuit for measuring force using *FlexiForce A201* sensor. $R_f = 20k\Omega$ [Source: Tekscan, Inc. (TekscanInc, 2007)

6.2.1.4 Experimental protocol

The aim of this experiment was to determine the performance of FD as measure of muscle properties. This experiment was performed to observe

- the change in FD when there is only small increase ($\approx$ 25% MVC) in muscle contraction
- the change in FD for different muscle groups with different complexities i.e., change in size and level of contraction.

At the start of the experiment, each participant was made to generate maximum voluntary contraction (MVC) for 10 seconds and this was repeated 5 times for each muscle. Based on the study (Basmajian and De Luca, 1985), the average of these five recordings was considered to be the MVC. MVCs were measured using the force sensor while maintaining the contraction and were calculated from the measured force prior to the recording of sEMG, when the participant were

asked to perform the high level contraction of the flexions. The average measured force in terms of voltage for different finger flexions have been tabulated in Table 6.2.

Table 6.2: Average Measured force in terms of volts for different finger flexions

Contraction	Average Measured Force (volts)
Quadriceps femoris	128.4mV
Biceps brachii	491mV
Flexor digitorium superficialis	783.2mV

Experiments were conducted where sEMG was recorded when participants were asked to maintain flexion from different muscles (Table 6.1) for 7-8 secs for three different levels of forces i.e., 20%, 50% and 80% of MVC. Each contraction was performed and repeated for the time period of 90 seconds. This protocol was repeated for two different sessions to obtain varied set of data for further analysis.

Table 6.3: Different level of contractions and its corresponding type number for the purpose of analysis.

Type No.	Name of the muscle and type of contraction
1	Quadriceps femoris - at 20% MVC
2	Quadriceps femoris - at 50% MVC
3	Quadriceps femoris - at 80% MVC
4	Biceps brachii - at 20% MVC
5	Biceps brachii - at 50% MVC
6	Biceps brachii - at 80% MVC
7	Flexor digitorum superficialis - at 20% MVC
8	Flexor digitorum superficialis - at 50% MVC
9	Flexor digitorum superficialis - at 80% MVC
10	Zygomaticus muscle- mild contraction
11	Zygomaticus muscle- medium contraction

6.2.2 Data Analysis

The first step of the data analysis required the computation of FD and MFL for recorded sEMG signal during each activation. A moving window with size of 1024 samples or one second was used to determine FD. FD was determined as mentioned in Section 5.3 for each moving window size to obtain the optimum data. The method to compute FD using moving window is shown in the Fig. 6.3.

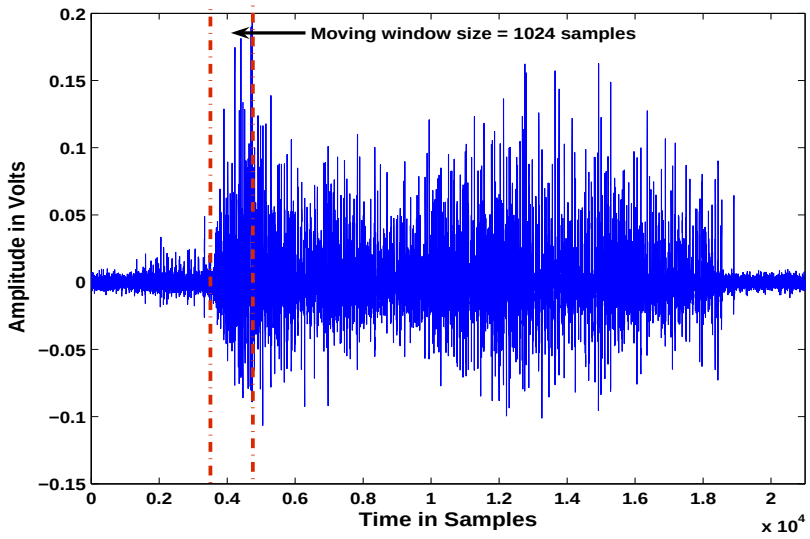

Figure 6.3: Computation of FD of sEMG using moving window size of 1024 samples

6.2.2.1 Statistical analysis of data

Analysis of variance (ANOVA) was conducted to determine the p-value to determine the significance in the relationship between

1. force of contraction and FD, and

2. FD and size of the muscle.

Fifty examples of each contraction were analysed (N = 50) from each participant. The statistical significance of the data was computed using ANOVA between the force of contraction and the value of FD. The results were then plotted on a box plot to determine the significance of the data. The boxplot is a quick graphic for examining one or more sets of data. Box plots (Chambers et al., 1983) are an excellent tool for conveying location and variation information in data sets, particularly for detecting and illustrating location and variation changes between different groups of data.

6.2.3 Observations - Performance of FD

The mean values and standard deviations (for 50 flexions) of RMS, MFL and FD of sEMG for all the experiments have been tabulated in Table 6.4. These results have also been displayed as a box plot in Fig.6.4.

Table 6.4: Average values (and standard deviation) of FD for the four muscles when undertaking 20%, 50% and 80% maximum voluntary isometric contraction.

Name of muscle	FD (mean ± SD)		
	20% MVC	50% MVC	80% MVC
Quadriceps	1.9947 ± 0.0004	1.9959 ± 0.0002	1.9966 ± 0.0001
Biceps	1.9609 ± 0.0002	1.9642 ± 0.0011	1.9749 ± 0.0012
FDS	1.9876 ± 0.0036	1.9889 ± 0.0056	1.9902 ± 0.0052
Zygomaticus muscle (Facial)	Type No.10 1.7660+0.001	Type No.11 1.7671+0.002	

It is observed from Table 6.4 that the value of FD is greater for larger and more complex muscles compared to smaller muscles. The mean FD for smaller

size muscle (facial) is less (FD = 1.7660) when compared with mean FD for larger size muscle (Quadriceps: FD = 1.9966). The results also indicate that there is a very small increase ($\approx 1\%$) in FD with increase in muscle activity for any given muscle. These results indicate that FD is a property of the muscle and not related to the muscle activity.

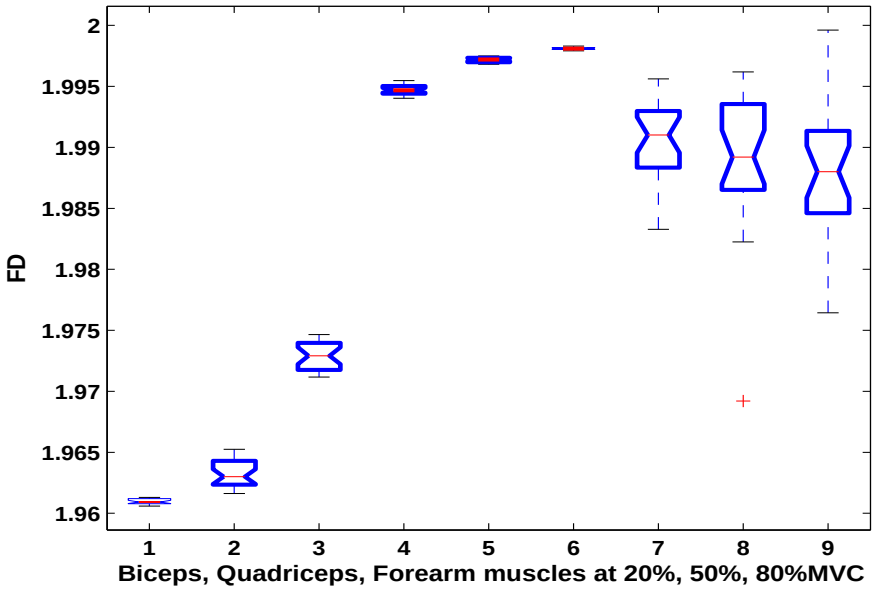

Figure 6.4: Boxplot for FD of sEMG for the muscle groups of different properties at various levels of force of contraction (20%, 50% and 80% MVC)

In order to validate these results, visualisation of ANOVA analysis of data was performed using the boxplot as shown in Fig.6.4. From the plot, it is observed that the fractal dimension varies with different muscle sizes and FD remains same even when there is small level of increase in muscle contraction for the same muscle. The boxplot clearly shows that same muscle group during different force levels of contraction lie in the same quartile range (QR), whereas the range differs with different muscle groups. This indicates the FD is a measure of overall muscle

property and can be used as an indicator of different sizes of muscle.

The results of this analysis demonstrate that

- larger and complex muscles have higher FD
- there is a very small ($\approx 1\%$) increase in FD with increase in muscle activity for a given muscle.

This experimental analysis validates that FD is measure of muscle property and not a measure of muscle activity when there is low-level muscle actvation. In order to determine the small changes in the muscle activity during low-level muscle activation, a new feature of Fractal analysis, Maximum fractal length(MFL), as explained in *Section 5.4* has been identified. The performance analysis of MFL as a measure of low-level muscle activation has been explained in the following section.

6.3 Experimental Analysis of performance of MFL as a measure of low level muscle activation

This section reports the performance analysis of MFL as a measure of the muscle activation. This experimental analysis was conducted to identify the relationship between MFL and the muscle activation. The aim of this analysis is to determine that MFL is a measure of low-level muscle activation and the performance of MFL was compared with that of RMS, which is a common measure of muscle activation.

6.3.1 Experimental Setup

The experimental setup was designed to record sEMG while performing subtle finger movements under various force levels of activation. This experimental model was used to analyse the performance of MFL as a measure of low-level muscle activation and was compared with RMS, which is a common mesaure of muscle activation. The number of participants and sEMG recording procedures for this experiment has been explained in *Section 6.2*.

6.3.1.1 Muscles Studied

In this experimental study, to determine the relationship between MFL and the muscle activation, low-level subtle movements were chosen. The finger flexions with the different force levels of subtle movements were considered for this study. In order to record sEMG performing these flexions, *Flexor digitorum superficialis (FDS)* muscle group in forearm was chosen due to its complexity and its function, based on the anatomical study. The function of FDS muscle is explained below (Marieb, 1997; Palastanga et al., 2006):

- Flexor digitorum superficialis (FDS)
  - Two-headed muscle; more deeply placed; overlain by muscles above but visible at distal end of forearm
  - Flexes wrist and middle phalanges of fingers 2-5; the important finger flexor when speed and flexion against resistance are required

6.3.1.2 Experimental protocol

This section discusses about the experimental protocol to determine the performance of MFL as measure of low-level muscle activity. The experimental protocol was designed to consider the different MVC for subtle movements. MVCs were measured as explained in *Section 6.2.1.3*. The different muscle groups of forearm were studied and Flexor digitorum superficialis (FDS) was found to be the appropriate muscle for subtle finger movements. FDS lies in the anterior compartment of the forearm, which has a primary function of flexing the digits in finger movements (Marieb, 1997; Palastanga et al., 2006).

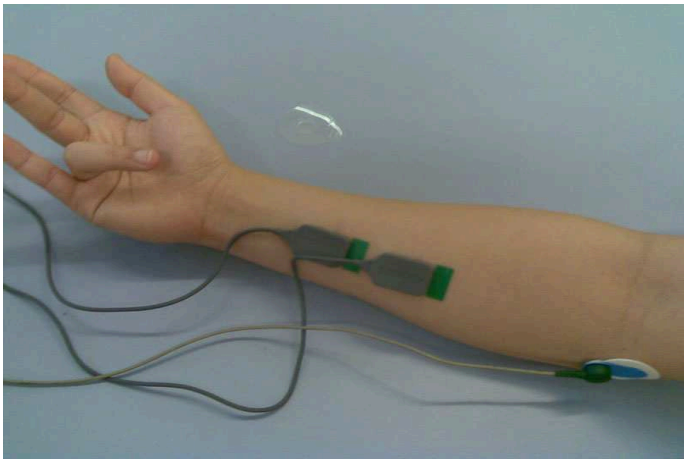

Figure 6.5: Placement of electrodes on surface of the forearm muscle

Experiments were conducted where sEMG from the Flexor digitorum superficialis (FDS) muscle was recorded when the participant maintained specific finger flexion. The two electrode channels were placed in the surface on FDS muscle. The electrodes placement on the forearm of the participant is shown in Fig. 6.5. The force of contraction was measured using FlexForce sensor. Three different finger flexions as shown in Fig.6.6 were used as protocol to record sEMG from

the participant:

- Middle finger flexion,
- Ring finger flexion and
- Little finger flexion

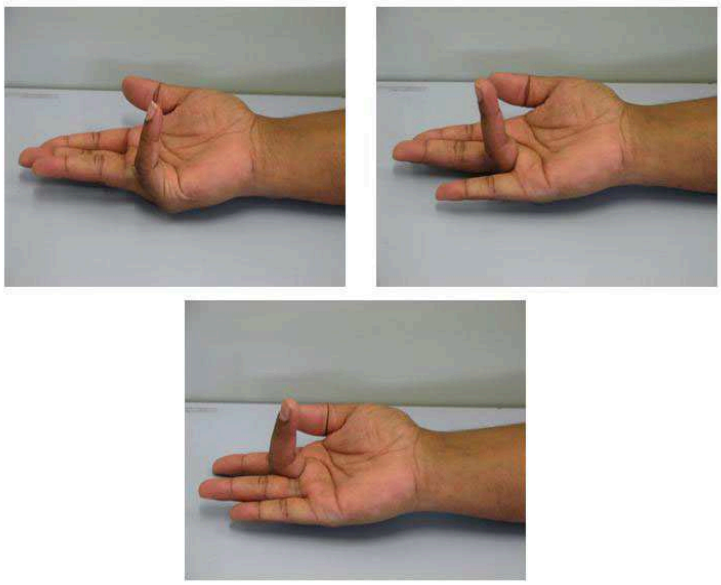

Figure 6.6: Three different finger flexions: Little, Ring, Middle, as performed by participants.

The participant was asked to maintain each flexion for 7-8 secs for three different levels of forces i.e., 20%, 50% and 80% of MVC. MVCs were calculated from the measured force prior to the recording of sEMG, when the participant were asked to perform the high level contraction of the flexions. The average measured force in terms of voltage for different finger flexions have been tabulated in Table 6.5.

The duration of each run of the flexion was 120 secs. Each flexion was repeated several times within the duration of 120 secs. The sampling rate for recording

Table 6.5: Average Measured force in terms of voltage for different finger flexions

Flexions	Average Measured force (in terms of voltage)
Little finger	95 mV
Middle finger	128.4 mV
Ring finger	194.2 mV

sEMG was 1024 samples/sec. To record the force exerted on the sensor, voltage across a fixed resistance in series with *FlexiForce* force sensor was recorded at 1024 samples/sec along with sEMG signal. The change in resistance of the *FlexiForce* is the measure of force of the sensor. Visual feedback of the force sensor output was given to the user to maintain steady muscle contraction.

6.3.2 Data Analysis

The analysis of the recorded of sEMG was performed to determine the suitability of using MFL as a measure of low-level muscle activity. The two steps were followed in the analysis of data:

- Computation of MFL and RMS for each flexion at different force levels.
- Statistical analysis to determine the relationship between force of contraction (% of maximum voluntary contraction) with MFL and with RMS to determine the signficance of these relationships.

The analysis of data in this research study were performed using MATLAB software.

6.3.2.1 Determining MFL and RMS of sEMG

The first step of this analysis is the computation of MFL value for each flexion using window size of 1024 samples or one second. MFL was computed as mentioned in *Section 5.4* for each moving window size to obtain the optimum data. Similarily, RMS for each flexion was calculated for the same window size using Eqn 6.1.

$$X_{rms} = \sqrt{\frac{1}{n}\sum_{i=1}^{n} x_i^2} \tag{6.1}$$

6.3.2.2 Statistical analysis of data

The results of the experiments were analyzed statistically to determine the significance of the data using student's t-test (95% confidence interval). Fifty samples (N = 50) of MFL of finger flexion for each finger were analysed for each participant. The statistical significance of the data was computed using sample t-tests between the force of contraction and the value of MFL. This was repeated for RMS of sEMG and force of contraction. The statistical analysis of the data from this experiment was conducted by computing the mean and standard deviation of MFL for the finger flexions during different levels of MVC. The p- value was computed to determine the significance of MFL of flexions with different maximum voluntary contractions (MVCs).

Student's t-Test is one of the most commonly used techniques for testing a hypothesis on the basis of a difference between sample means. Explained in layman's terms, the t-test determines a probability that two populations are the same with respect to the variable tested. If the calculated p-value is below the

threshold chosen for statistical significance (usually the 0.05 level), then the null hypothesis which usually states that the two groups do not differ is rejected in favour of an alternative hypothesis, which typically states that the groups do differ. The results were then plotted on a box plot to visualise the significance of the data. The boxplot provides an excellent visual summary of many important aspects of a distribution. They are particularly useful for comparing distributions between several groups or sets of data.

6.3.3 Observations - Performance of MFL and RMS

The performance of MFL as a measure of low-level muscle activation and its comparison with RMS were observed using the following summarised Tables:

- The mean values (for 50 samples) of RMS and MFL of sEMG for the three different finger flexions at the three different levels of strength of contraction for each participant have been tabulated in Table 6.6.
- The *p values* of the two sample t-tests as a measure of the significance of the relationship of MFL and RMS of sEMG with strength of muscle contraction for the different participants have been tabulated in Table 6.7.

The values of MFL were compared with the RMS for different flexions at different MVCs, to determine the measure of low-level muscle activation.

6.3.3.1 Comparative results using Statistical analysis

MFL (the fractal feature) and RMS were compared for their performance by determining the significance of separation of each flexions corresponding to different force levels of contraction. The results were summarised in Table 6.6 and Table

6.7. From Table 6.6, it is observed that there is large increase in mean MFL values for different finger flexion as the force of contraction increases from 20% MVC to 80% MVC($\approx$ 125%) for all subjects. But the mean values of RMS have a marginal increase or no increase as the force of contraction increases from 20% MVC to 50% MVC. From Table 6.6 and Table 6.7, it is observed that MFL is a

Table 6.6: Mean values of MFL and RMS values for different flexions (L - Little finger; R - Ringer finger; M - Middle finger) under different force (%MVCs)

		20% MVC		50% MVC		80% MVC	
	Flexions	MFL	RMS	MFL	RMS	MFL	RMS
Subject 1	L	5.12	0.033	6.72	0.031	7.44	0.042
	R	31.60	0.088	33.46	0.082	62.36	0.084
	M	43.20	0.085	52.44	0.074	75.73	0.100
Subject 2	L	4.90	0.047	5.27	0.021	8.12	0.055
	R	25.27	0.063	26.46	0.081	43.36	0.096
	M	35.31	0.069	42.44	0.092	55.56	0.150
Subject 3	L	6.84	0.032	7.62	0.032	7.71	0.039
	R	30.76	0.058	36.08	0.056	68.91	0.088
	M	42.15	0.065	52.88	0.069	89.35	0.114
Subject 4	L	5.76	0.052	6.70	0.048	10.74	0.051
	R	21.16	0.062	28.45	0.065	58.57	0.094
	M	36.58	0.072	41.44	0.084	70.75	0.141
Subject 5	L	8.11	0.047	7.72	0.046	15.44	0.066
	R	29.41	0.068	40.41	0.052	73.35	0.101
	M	50.31	0.076	58.47	0.074	105.71	0.180

good indicator of strength of muscle contraction. The results show that values of MFL are a good indicator of the force of contraction of the muscles for all levels of muscle contraction.

RMS of sEMG is an indicator of the force of contraction only when the level of contraction is high (80% MVC) but a poor indicator of the force of contraction

Table 6.7: p values from t-test for five subjects. The pairs of samples are: L-R:Little and Ring finger flexion, R-M:Ring and Middle finger flexion, and L-M:Little and Middle finger flexion

		20% MVC		50% MVC		80% MVC	
	Flexions	MFL	RMS	MFL	RMS	MFL	RMS
Subject 1	L-R	0.0001	0.001	0.0001	0.0001	0.0001	0.0001
	R-M	0.001	0.914	0.0001	0.195	0.0001	0.011
	L-M	0.0001	0.0001	0.0001	0.0001	0.0001	0.0001
Subject 2	L-R	0.0001	0.0001	0.0001	0.0001	0.0001	0.0001
	R-M	0.001	0.294	0.001	0.104	0.0001	0.001
	L-M	0.0001	0.001	0.0001	0.0001	0.0001	0.0001
Subject 3	L-R	0.0001	0.001	0.0001	0.0001	0.0001	0.0001
	R-M	0.001	0.404	0.001	0.21	0.0001	0.01
	L-M	0.0001	0.0001	0.0001	0.0001	0.0001	0.0001
Subject 4	L-R	0.0001	0.001	0.0001	0.0001	0.0001	0.0001
	R-M	0.001	0.510	0.001	0.011	0.0001	0.01
	L-M	0.0001	0.001	0.0001	0.0001	0.0001	0.0001
Subject 5	L-R	0.0001	0.0001	0.0001	0.0001	0.0001	0.0001
	R-M	0.001	0.32	0.001	0.136	0.0001	0.0001
	L-M	0.0001	0.001	0.0001	0.0001	0.0001	0.0001

when the level of contraction is low (20%). This may be attributable to the effect of the background actvity during low-level muscle activity. The increase in the value of MFL of sEMG corresponding to 30% increase in MVC was of the order of 200% while there was no significant increase in the value of RMS and in number of cases RMS value decreased with increase in the strength of muscle contraction.

In order to validate and visualise the data, the values were plotted using boxplot to determine the difference in MFL for flexions during different levels of contraction. Boxplots can be useful to display differences between populations without making any assumptions of the underlying statistical distribution. The

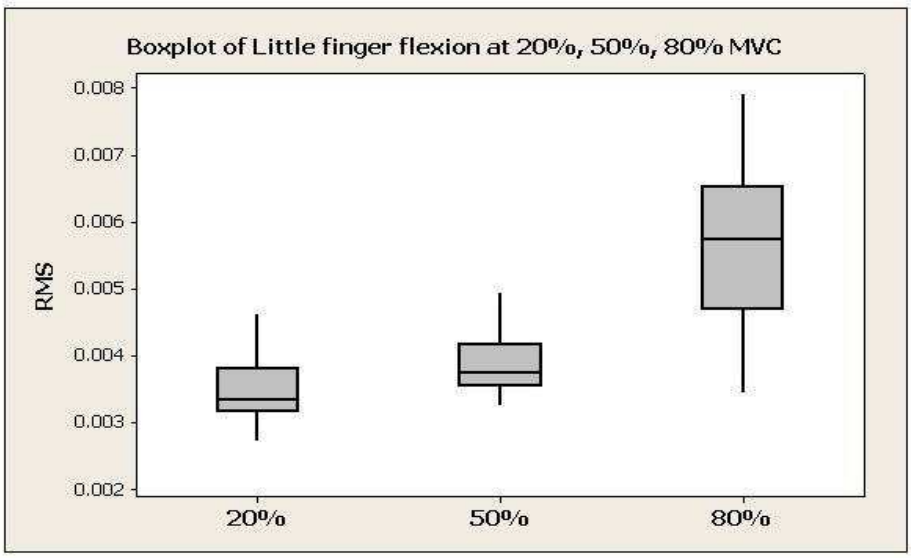

Figure 6.7: Boxplot for RMS of sEMG for the Little finger flexion at 3 different levels of force of contraction

space between the different parts of the box help indicate the degree of dispersion (spread) and skewness in the data, and identify outliers.

The boxplots for RMS and MFL of sEMG for the flexion of the little finger at the three different levels of force of contraction for Subject 1 are shown in Fig.6.7 and Fig.6.8 respectively. From these plots, it is observed that MFL is reliably able to differentiate between force of finger flexion - 20%, 50% and 80% MVC while this is not possible using RMS of sEMG.

Similarly, the plots for the Ring and Middle fingers flexion shown in Fig.6.9, Fig.6.10, Fig.6.11 and Fig.6.12, indicate that MFL has more signifcant change than RMS, during low-level flexions with respect to the force levels of contraction.

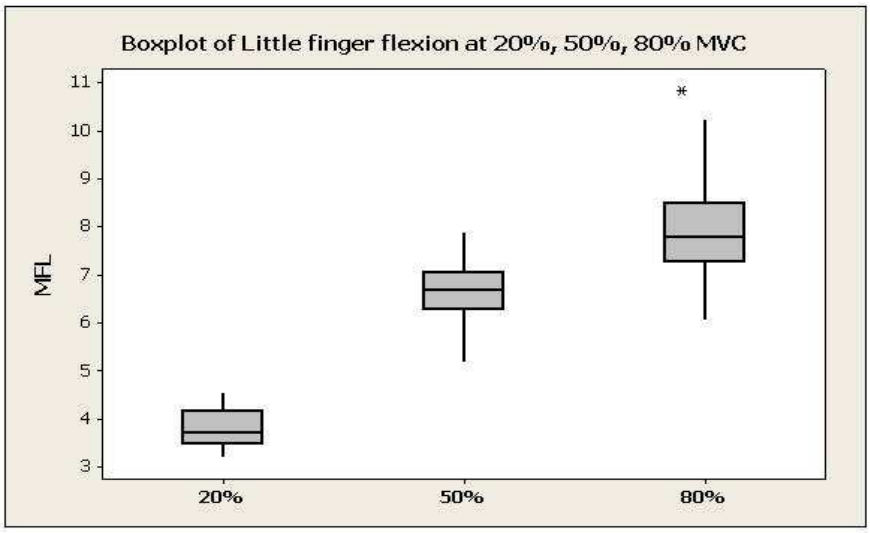

Figure 6.8: Boxplot for MFL of sEMG for the Little finger flexion at 3 different levels of force of contraction

6.4 Discussion - performance of FD and MFL

The physiological relationship between FD and MFL with sEMG, as explained in *Section 5.3* and *Section 5.4* respectively has been observed and evaluated in this performance analysis. It is observed from the results that FD is a measure of muscle property and not a measure of low-level muscle activation. The mean value of FD varied increasingly for different properties of muscles and remained same even for low-level increase in muscle activation (refer Table 6.4). This performance study has concluded that FD is not dependent on the strength of muscle contraction but on the muscle properties such as size and complexity. For small variations in muscle contraction, there is very small change in the value of FD ($\approx 1\%$) while there is a significant change in MFL ($\approx 200\%$). The study has also demonstrated that FD is dependent on the size and complexity of the active muscles, with the value of FD being higher for larger muscles, or when

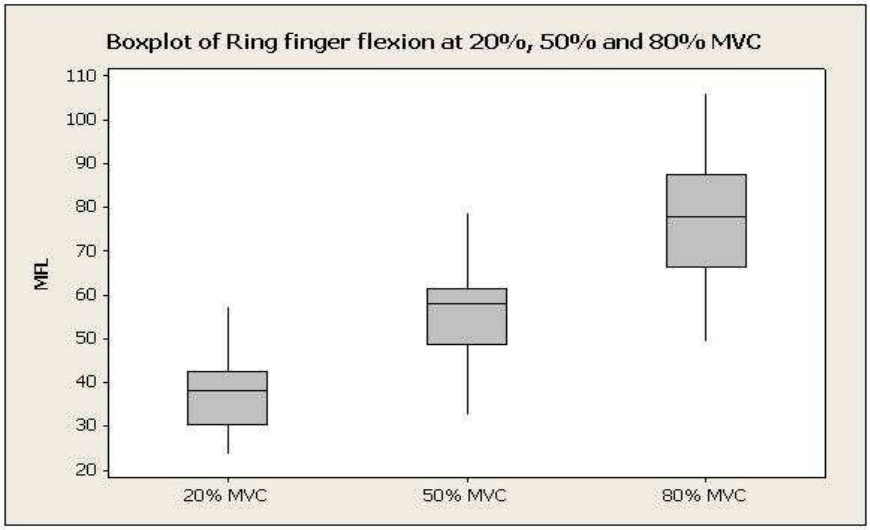

Figure 6.9: Boxplot for MFL of sEMG for the Ring finger flexion at 3 different levels of force of contraction

there are multiple simultaneously active muscles. Based on this experimental study, the results suggest that the observed change in FD with strength of muscle contraction is a result of changes in muscle properties due to high levels of muscle contraction and associated movement or change in length.

The performance of the new feature of fractal, MFL as a measure of low-level muscle activation was evaluated and compared with RMS, a common feature for the measure of sEMG. Statistical comparison of the relationship of MFL and RMS with strength of contraction indicates that MFL is a significantly better measure of muscle activity than RMS for all levels of muscle contraction. When the level of contraction is less than 50%, RMS does not appear to be a good measure of contraction ($p < 0.05$) while MFL is a good measure even when the strength of contraction is only 20% MVC ($p < 0.001$).

MFL is a measure of wavelength from the fractal plot and due to the logarith-

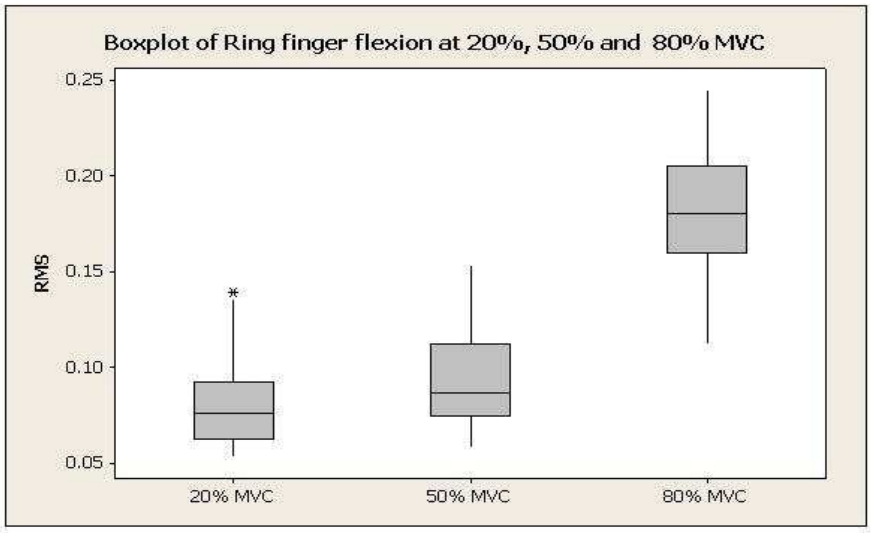

Figure 6.10: Boxplot for RMS of sEMG for the Ring finger flexion at 3 different levels of force of contraction

mic nature, only the singularities have a significant impact on this value while the background activity is ignored and is less sensitive to noise. MFL is thus related to the density of singularities in the signal and in the case of sEMG, it is related to the density of MUAPs.

It is observed that there is a close relationship between the muscle activity and MFL - *MFL increases with increase in the muscle activity.* The results demonstrate that MFL is suitable for measuring force of muscle contraction while at low levels of muscle contraction RMS is not suitable. At low levels of contraction RMS of sEMG of the relaxed muscle and contracting muscle is comparable. This performance evaluation study determined the strengths of fractal features (MFL, FD). This suggests that these features can be used in the identification of small changes and properties in biosignals.

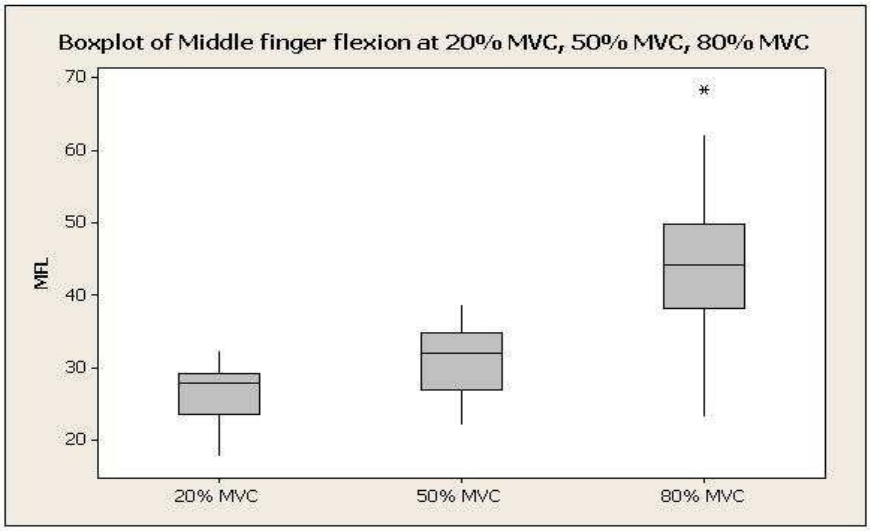

Figure 6.11: Boxplot for MFL of sEMG for the Middle finger flexion at 3 different levels of force of contraction

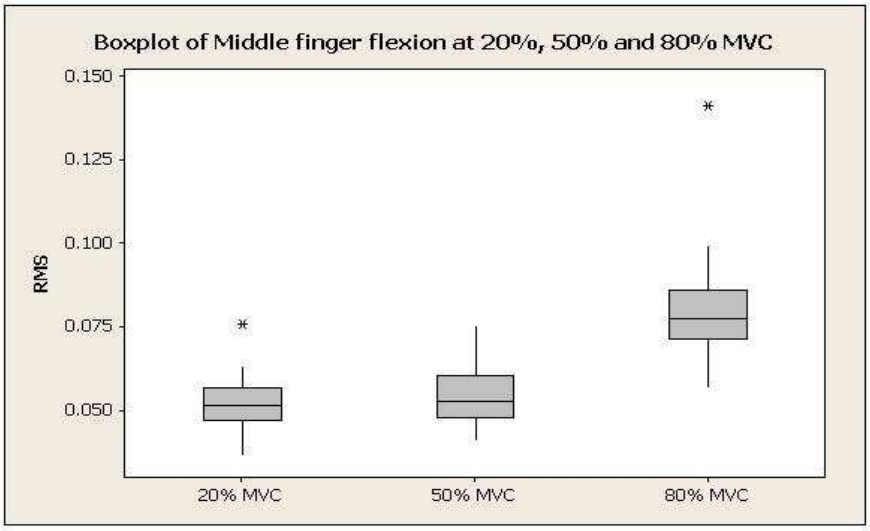

Figure 6.12: Boxplot for RMS of sEMG for the Middle finger flexion at 3 different levels of force of contraction

Chapter 7

Application - Performance analysis of Fractal features (MFL,FD) of sEMG and EEG

7.1 Introduction

This chapter proposes and experimentally verifies the efficacy of MFL and FD of biosignals for real-time applications. In this study, the following two applications are examined:

- Identification of wrist and finger flexions using single channel sEMG and
- Identification of changes in EEG recording in response to alertness levels

The outcome of the experiments were statistically analysed to determine the reliability of separation. The data was also classified using an artificial neural network based (ANN) classifier. Each of these are described in the following

sections.

7.2 Identification of Subtle finger and wrist movements using FD & MFL of single channel sEMG

In this section, the performance of fractal features in identifying low-level or subtle movements has been analysed. To verify this experimentally, wrist and finger flexions were considered that has a wide applications in prosthetic control and a number of other rehabilitation applications. Most sEMG based control systems that are currently available, extract control information from sEMG signal based on an estimate of the amplitude (Lowery and O'Malley, 2003) or the rate of change (Falla et al., 2007) of the muscle activity. Even though these systems have been successful, general limitation of these techniques is that these are unsuitable at low levels of contraction. There is a need of reliable control for multiple functions (or device) or for subtle functions (Costanza et al., 2005).

Experiments were conducted where sEMG was recorded during predefined actions. The fractal features, FD & MFL of single channel recording were compared with RMS of multiple channels. The experimental verification of using the feature set of FD and MFL for identifying small finger and wrist flexion has been reported in this section. The data were classified to determine the ability of using a combination of FD and MFL from only one channel to recognize the finger and wrist flexion actions.

7.2.1 Experimental setup

The experimental setup design included the selection of wrist and finger flexions based on the anatomical study of muscle groups which relate to different forearm flexions.

7.2.1.1 Muscle studied

Four muscle groups in forearm were chosen for this study: *Brachioradialis, Flexor Carpi Radialis (FCR), Flexor Carpi Ulnaris (FCU), Flexor digitorum superficialis (FDS)*. These muscles play an important role in wrist and finger flexion movements (Marieb, 1997; Palastanga et al., 2006). A brief description and action of each muscle is explained below:

- Brachioradialis
  - Superficial muscle of lateral forearm; extends from distal humerus to distal forearm
  - Synergist in forearm flexion; acts to best advantage when forearm is partially flexed and semi-pronated
- Flexor Carpi Radialis (FCR)
  - Runs diagonally across forearm; midway, its fleshy belly is replaced by a flat tendon that becomes cordlike at wrist
  - Powerful flexor of wrist; abducts hand; synergist of elbow flexion
- Flexor Carpi Ulnaris (FCU)

- Most medial muscle of this group; two headed; ulnar nerve lies lateral to its tendon
- Powerful flexor of wrist; stabilizes wrist during finger flexion.

- Flexor digitorum superficialis (FDS)
  - Two-headed muscle; more deeply placed; overlain by muscles above but visible at distal end of forearm
  - Flexes wrist and middle phalanges of fingers 2-5; the important finger flexor when speed and flexion against resistance are required

7.2.1.2 Experimental protocol

The experimental protocol was designed to determine the performance of FD & MFL as a feature set for identification of subtle wrist and finger actions. SEMG recording and processing were followed as explained in *Section 6.2*.

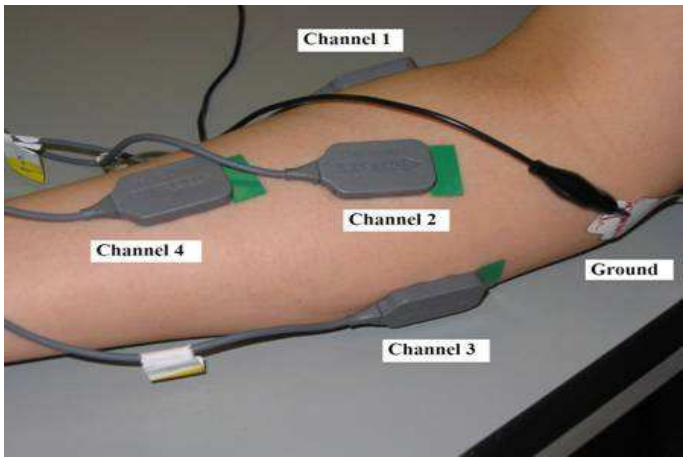

Figure 7.1: Placement of electrodes and description of channels

Four pairs of electrodes were placed on the forearm muscles on four muscle groups as shown in Fig.7.1. Table 7.1 shows the channel number and its associ-

ated muscle used for this experimental recording. Experiments were conducted where sEMG from the four electrode pairs were recorded when the participant maintained specific wrist and finger flexion (Table 7.2).

Table 7.1: Channel Number and its associated muscle

Channel Number	Associated muscle
1	Brachioradialis
2	Flexor Carpi Radialis (FCR)
3	Flexor Carpi Ulnaris (FCU)
4	Flexor digitorum superficialis (FDS)

The data analysis was performed considering all channel recordings and compared with the performance of fractal feature of sEMG from only Channel 2. This channel was chosen because it is closest to the elbow and most suitable for helping people with hand amputation.

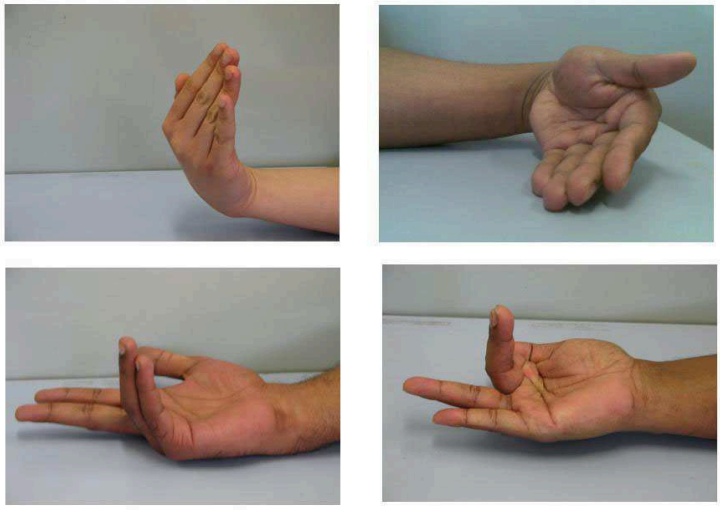

Figure 7.2: Four different wrist and finger flexions used in this experimental protocol (Table 7.2)

The four different wrist and finger flexions used in this experimental protocol

were numbered as shown in Table 7.2. The participants were asked to maintain each flexion (as shown in Fig. 7.2) for 7-8 secs for three different levels of forces. Each flexion was repeated several times within the total duration of 120 secs.

Table 7.2: Flexion and its corresponding flexion number

Flexion Number	Flexion
G1	Wrist flexion (Basal)
G2	Index and Middle finger flexion
G3	Wrist flexion (Lateral)
G4	Little and ring finger flexion

7.2.2 Data Analysis

As the first step of the analysis, the fractal features, FD and MFL, of the recorded sEMG were determined from the procedure explained in *Chapter 4*. The calculated fractal features were analysed to demonstrate the ability of this feature set to identify the different actions using sEMG and compared with RMS based techniques reported in literature (Costanza et al., 2005; Momen et al., 2007).

The analysis of data for its reliability and significance in separation was divided into following three parts:

- Scatter plot analysis of data
- Statistical significance analysis using MANOVA
- Classification of data using Artificial Neutral Network (ANN) classifier

7.2.2.1 Visualisation using Scatter plot

A scatter plot, also called a scatter diagram or a scattergram, is a basic graphic tool that illustrates the relationship between two variables. The dots on the scatter plot represent data points. Scatter plots are used with variable data to study possible relationships between two different variables. In this data analysis, as a first step, the fractal features of single channel were visualised to determine the separation of classes related to the different subtle movements. The scatter plot MFL and FD for the data from the Channel 2 is shown in Fig.7.3.

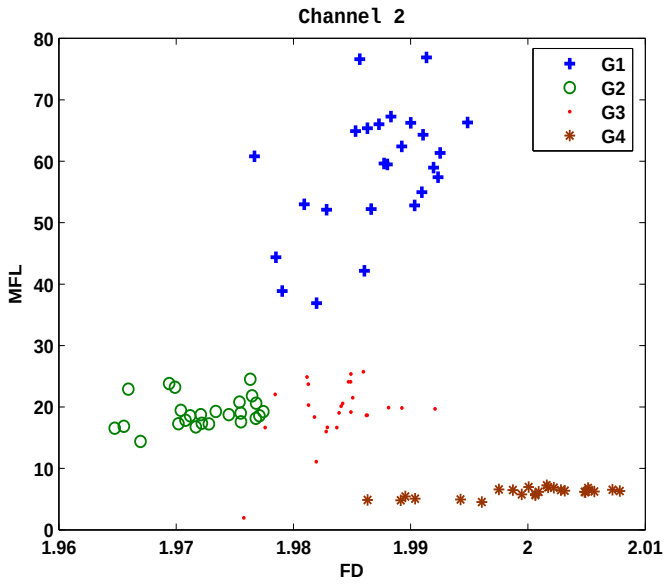

Figure 7.3: Scatter plot of FD and MFL of single channel (Channel 2) for different subtle movements

From the plot (Fig.7.3), it is visualised that the different clusters of data points are related to different classes. Even though a scatter plot depicts a relationship between variables, it does not indicate a cause and effect of the relationship. Statistical analysis was performed to examine the significance of this relationship.

7.2.2.2 Statistical analysis using MANOVA

Multi-variate analysis of variance (MANOVA) was conducted to determine the significance of the data separation. MANOVA is an extension of One-Way Analysis of Variance (ANOVA). It analyzes the means of multiple variables to determine whether the mean of these variables differ significantly between classes. It measures the differences for two or more metric dependent variables based on a set of categorical variables acting as independent variables (Hair et al., 2006). To calculate the significance of the relatioships, the F value from the MANOVA table was used.

- **A Brief about F-test**

An F-test is a statistical test in which the test statistic has an F-distribution if the null hypothesis is true. Sir Ronald A. Fisher initially developed the statistic as the variance ratio in the 1920s (Fisher, 1922). Consider the two different models (simpler and complicated) for analysis in F-test. If the simpler model is correct, the relative increase in the sum of squares (going from more complicated to simpler model) is expected to equal the relative increase in degrees of freedom (GraphPad, 2007; Lomax, 2001). If the simpler model is correct it is expected that:

$$(SS1 - SS2)/SS2 \approx (DF1 - DF2)/DF2 \tag{7.1}$$

where SS1 is the sum-of-squares for the simpler model (which will be higher) and SS2 is the sum-of-squares of the more complicated model. If the more complicated model is correct, then it is expected that the relative increase in sum-of-

squares (going from complicated to simple model) to be greater than the relative increase in degrees of freedom:

$$(SS1 - SS2)/SS2 > (DF1 - DF2)/DF2 \tag{7.2}$$

The F ratio quantifies the relationship between the relative increase in sum-of-squares and the relative increase in degrees of freedom.

$$F = \frac{(SS1 - SS2)/SS2}{(DF1 - DF2)/DF2} \tag{7.3}$$

That equation is more commonly shown in an equivalent form:

$$F = \frac{(SS1 - SS2)/(DF1 - DF2)}{SS2/DF2} \tag{7.4}$$

F ratios are always associated with a certain number of degrees of freedom for the numerator and a certain number of degrees of freedom for the denominator. This F ratio has DF1-DF2 degrees of freedom for the numerator, and DF2 degrees of freedom for the denominator. The p-value, which is derived from the *cdf* of F, determines the significance of the separation and as F increases, the p-value decreases.

Canonical analysis was performed on MANOVA to identify the variables that provide the most significant separation between groups (Hair et al., 2006). Canonical variables are linear combinations of the mean-centered original variables. Twenty-five examples of wrist and finger flexion for each movement were analyzed (N = 25) for each participant. The significance of the data was computed for the feature set combining FD and MFL and was repeated for RMS values for

comparison.

7.2.2.3 Classification Using ANN

The aim of the classification was to determine the ability of the system to identify the different actions using sEMG. Neural network is a general purpose non-linear classifier that can be iteratively trained using examples. This was used for the purpose of classification to compare the proposed technique with the other techniques reported in literature that are based on RMS of sEMG. For the sake of comparison, RMS of the same recordings were also classified using a similar neural network. A simple multilayer perceptron (MLP) artificial neural network (ANN) was used for the classification of the features (Freeman and Skapura, 1991).

Supervised artificial neural network (ANN) approach lends itself for identifying the separability of data even when the statistical properties and the types of separability (linear or nonlinear) are not known. A feed forward MLP ANN classifier with back propagation (BP) learning algorithm is used in this approach.

The ANN architecture used for this analysis consisted of two hidden layers with a total of 20 nodes in both the layers with sigmoid function as the threshold decision. The training and testing was done using this designed ANN architecture with back propagation algorithm using a momentum with a learning rate of 0.05 to reduce the likelihood of local minima. The training and testing data were orthogonal sets and membership was randomly allocated from the experimental data. To compare the proposed technique with other techniques (Momen et al., 2007), RMS of all the four channels and for two channels were also analysed using a similar approach as above.

7.2.3 Observations - Performance of Fractal features (MFL and FD)

The results from the data analysis were observed and reported in this section to validate the performance of the fractal features. The scatter plot in Fig.7.3 visualises the separation of different classes pretaining to subtle movements using MFL and FD. This confirms the formation of the fractal features into clusters corresponding to the different gestures. The significance of this separation were observed from the results of statistical MANOVA analysis.

From the grouped scatter plot (shown in Fig.7.4) for first two canonical variables from MANOVA analysis of 4 channel RMS values, it is observed that there appear to be clusters but there is substantial amount of noise. This confirms RMS is not reliable in identification of movements when the muscle activity is very subtle and when there are multiple active muscles for a particular activity. From Fig.7.5, it is observed that there are cluster formations of single channel sEMG using FD & MFL as features and for the four different finger & wrist flexions. This is confirmed from the statistic F value (Table 7.3).

The results of MANOVA on the fractal features produce the estimated dimension (d) of the class means of 3 for this fractal features. This indicates that the class means fall in a 3-dimensional space, which is the largest possible dimension for four classes. This demonstrates that the 4 class means are different. If the means of the classes are all the same, the dimension, d, would be 0, indicating that the means are at the same point. The *p-value* to test if the dimension is less than 3 ($d < 3$) is very small, $p < 0.0001$. This is confirmed from the MANOVA F-test table (Table 7.3) and shows that there is significant separation for the four

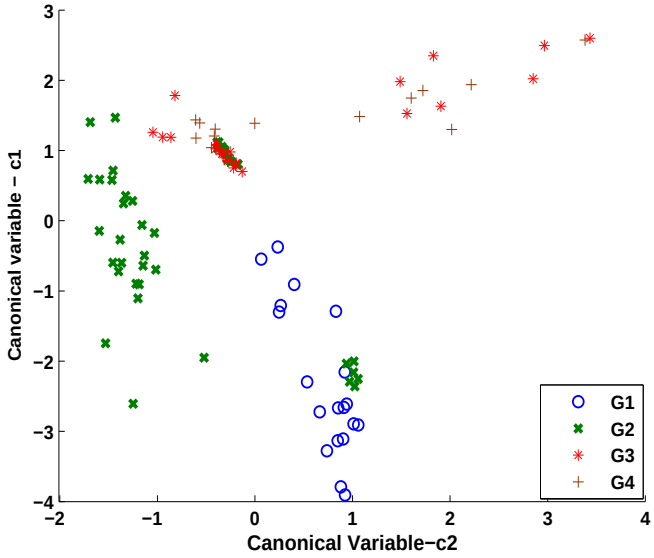

Figure 7.4: Grouped Scatter plot of first two canonical variables of RMS of four sEMG channels (Participant 1)

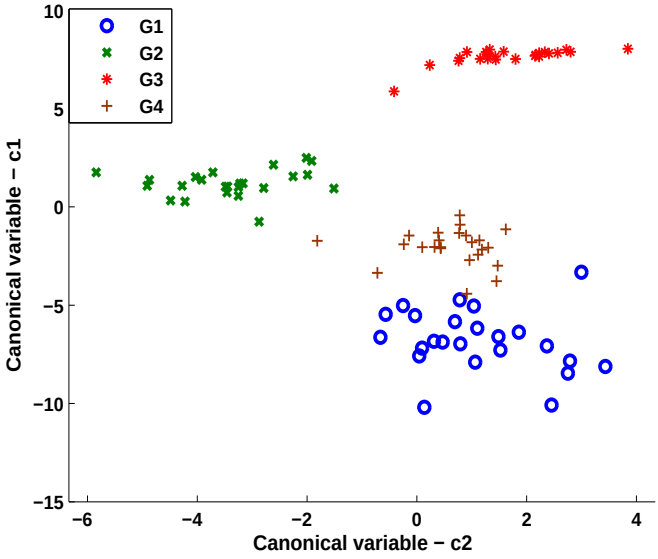

Figure 7.5: Grouped Scatter plot of first two canonical variables of MFL and FD of single sEMG channel (Participant 1)

actions where

- $p = 0.0001$ when using FD and MFL of single channel sEMG,
- $p = 0.054$ when using RMS of four channels sEMG and
- $p = 0.17$ when using RMS of two channels sEMG.

Table 7.3: F statistic value from MANOVA table for a) single channel MFL & FD b) RMS - 4 channels c) RMS - 2 Channels for four different wrist and finger flexions

	F		
Subjects	FD and MFL	RMS 4 channels	RMS 2 channels
Subject 1	144.133	20.915	16.213
Subject 2	156.346	23.336	22.436
Subject 3	240.467	22.126	18.342
Subject 4	324.326	21.985	19.564
Subject 5	189.434	22.568	23.233
Average p	0.0001	0.054	0.1676

From these results, it is obvious that using FD and MFL features of only one channel of sEMG, it is possible to identify each of the four different finger and wrist flexion actions, even when the level of activity is very low. The reliability of separation of the classes was first confirmed based on MANOVA and the data were then classified using the designed ANN architecture.

The recognition accuracy was calculated using the number of correctly classified fractal feature set from the test feature set values for the corresponding subtle actions. This analysis was repeated using the RMS feature from four channels and two channels sEMG.

The recognition accuracy for MFL and FD of single channel as feature set and for 4 channels and 2 channels of RMS are tabulated in Table 7.4, Table 7.5

Table 7.4: Recognition accuracy (FD and MFL) for different gestures (single Channel data) using ANN classifier

	Recognition accuracy			
Subjects	G1	G2	G3	G4
Subject 1	95.83	95.83	100	100
Subject 2	95.83	100	95.83	91.67
Subject 3	95.83	95.83	100	100
Subject 4	91.67	95.83	100	95.83
Subject 5	91.67	95.83	100	95.83

and Table 7.6 respectively. These tables indicate that the technique using fractal features identifies different finger and wrist movements with higher accuracy than using four channels and two channels RMS as features.

Table 7.5: Recognition accuracy (RMS) for different gestures (4 Channel data) using ANN classifier

	Recognition accuracy			
Subjects	G1	G2	G3	G4
Subject 1	86.67	86.67	86.67	86.67
Subject 2	86.67	86.67	80	80
Subject 3	80	86.67	66.67	66.67
Subject 4	86.67	80	86.67	66.67
Subject 5	86.67	80	80	80

The average accuracy of identification of the actions using neural network approach based on three different inputs is shown in Table 7.9. These results also reconfirm the above observation that MFL and FD of single channel is able to accurately identify the actions with 96.67% accuracy, while RMS of four channels gives an accuracy of 81.33% and RMS of two channels only 75%.

These results indicate that a combination of FD and MFL of only one channel

Table 7.6: Recognition accuracy (RMS) for different gestures (2 Channel data) using ANN classifier

	Recognition accuracy			
Subjects	G1	G2	G3	G4
Subject 1	86.67	86.67	66.67	66.67
Subject 2	86.67	86.67	66.667	66.67
Subject 3	86.67	80	60	66.67
Subject 4	80	86.67	66.67	60
Subject 5	86.67	80	66.67	66.67

sEMG can be used to identify each of the four different finger and wrist flexion actions. The classification accuracy using single channel MFL and FD were compared with the RMS of four channels or two channels sEMG and it shows that RMS is not reliable in identifying the different actions.

Table 7.7: A comparison between the % accuracy of identifying the correct action based on sEMG using the three techniques; (i) FD and MFL of single channel sEMG, (ii) RMS of 4 channel sEMG, and (iii) RMS of 2 channel sEMG. ANN was used for classification in each case.

	FD and MFL one channel	RMS 4 channels	RMS 2 channels
Average	96.67%	81.33%	75%
Standard deviation	2.04	4.21	11.17

7.3 Alertness level measurement using MFL & FD of EEG

Alertness deficit is a major problem where the operator is monitoring powered equipment or is responsible for control of complex situations. It can lead to

catastrophic consequences for people driving a car, monitoring power plant, and for air traffic controllers. Number of studies in past have shown that retaining a constant level of alertness is difficult or impossible for operators of motorized systems. Research studies (Bullock et al., 1995; Chapotot et al., 1998; Grigg-Damberger et al., 2007; Makeig and Inlow, 1993; Silber et al., 2007; Tassi et al., 2006) have shown the relationship of Electroencephalogram (EEG) with changes in alertness, arousal, sleep and cognition .

Electroencephalogram (EEG) is the recording of the electrical activity in the brain. Study by Jung et al. (Jung et al., 1997) has estimated alertness of people using power spectrum of EEG. One shortcoming with biosignals such as EEG is the very low signal to noise ratio. The typical signal strength of EEG signal is of the order of 1 micro-volt, and often the strength of artefacts and noise may be much greater than this. Artefacts such as electro-ocular gram (EOG) can often be an order of magnitude greater, making the use of EEG for automated analysis difficult and unreliable.

Researchers have reported that EEG waveforms corresponding to different physio pathological conditions can be characterized by their complexity (Accardo et al., 1997; Beckers et al., 2006; Durgam et al., 1997). One measure of complexity of a signal is the fractal dimension (FD), which is a global property of the signal. Recent studies by researchers (Accardo et al., 1997; Beckers et al., 2006; Durgam et al., 1997; Paramanathan and Uthayakumar, 2008; Zhonggang and Hong, 2006) have demonstrated the fractal nature of EEG. These studies have determined changes in FD with various levels of handgrip force. Studies reported in previous chapters has determined the fractal properties of sEMG. This section reports the performance of these fractal features (MFL & FD) of EEG in alertness level

measurement.

7.3.1 Experimental setup

The EEG experiment was conducted at Swartz centre and have been reported in publications (Jung et al., 1997; Makeig et al., 1996). These experimental data were obtained from Swartz Center for Computational Neuroscience, Institute for Neural Computation, University of California, San Diego and has been acknowledged. The experimental setup explained in this section has been obtained with permission from their publications (Jung et al., 1997; Makeig et al., 1996).

7.3.1.1 Subjects

Three healthy subjects (aged from 18 to 34) participated in a dual-task simulation of auditory sonar target detection. All had passed the standard Navy hearing tests or reported having normal hearing. Each subject participated in three or more simulated work sessions that lasted 28 minutes. Each participant was given an oral and written summary of the experimental protocol.

7.3.1.2 Stimuli

Auditory signals, including background noise, tone pips, and noise burst targets, were synthesized using a Concurrent work station which was also used to record the EEG. In a continuous 63 db white noise background, task-irrevalant auditory tones at two frequencies (568Hz and 1098 Hz) were presented in random order at 72dB (normal hearing level) with stimulus onset asynchronies between 2-4s. These signals were introduced to assess the information available in event-related potentials (Venturini et al., 1992), and are not reported in this study. In half

of the inter-tone intervals, target noise bursts were presented at 6dB above their detection threshold and the mean target rate was thus 10 per minute.

7.3.1.3 EEG recording and processing

EEG data were recorded at a sampling rate of 312.5 Hz from two midlines sites, one central (Cz) and other midway between parietal and occipital sites (Pz/Oz), using 10 mm gold-plated electrodes located at sites of the Inernation 10-20 system, referenced to the right mastoid. EEG data were first preprocessed using a simple out-of-bounds test (with a $\pm 50 \mu V$ threshold) to reject epochs that were grossly contaminated by muscle and /or eye-movement artifacts. Moving averaged spectral anlysis of the EEG data was then accomplished using a 256-point Hanning-window with 50% overlap. Windowed 256-point epochs were extended to 512 points by zero-padding. Median filtering using a moving 5s window was used to further minimize the presence of artifacts in the EEG records. Two sessions from each from the three of the participants were chosen for analysis on the basis of their including more than 50 detection lapses.

7.3.1.4 Experimental procedure

Experimental procedure was designed in order to determine the level of alertness from EEG recordings. Each subject participated in three or more 28-min experimental sessions on separate days. During the experiment, the participants mimicked audio sonar target detection. The participants were asked to respond to given auditory commands. The subjects pushed one button whenever they detected an above-threshold auditory target stimulus (a brief increase in the level of the continously-present background noise). To maximise the chance of observ-

ing alertness decrements, sessions wer conducted in a small, warm and dimly-lit experimental chamber, and subjects were instructed to keep their eyes closed.

7.3.1.5 Alertness Measure

Auditory targets were classified as *Hits* or *Lapses* depending on whether or not the subject pressed the auditory response button within 100 ms to 3000 ms of target onset. To quantify the level of alertness, auditory responses were converted into *local error rate*, defined as fraction of targets not detected by the subject (i.e., lapses) within a moving time window. A continuous measure, local error rate, was computed by convolving an irregurlarly spaced performance index (hit = 0/ lapse = 1) with a 95 s smoothing window advanced through the performance data in 1.64s steps. Each error rate time series consisted of 1024 points at 1.64 s intervals. Error rate and EEG data from the first 95 s of each run were not used in the analysis. For each window position, the sum of window values at moments of presentation of undeteced (lapse) targets was divided by the sum of window values at moments of presentation of all targets. The window was moved through the session in 1.64s steps, converting the irregularly-sampled, discontinuous performance record into a regularly-sampled, continuous error rate measure within the range [0,1].

7.3.2 Data Analysis

MFL and FD were computed from the EEG data using a stepping window of 1.64 s and were analysed to determine the correlation with the local error rate. The results of the experiments were analyzed to determine the alertness levels in relation to the small changes in EEG using the correlation analysis.

7.3.2.1 Correlation Analysis

Correlation analysis often measured as a correlation coefficient, it indicates the strength and direction of a linear relationship between two random variables. In general statistical usage, correlation or co-relation refers to the departure of two variables from independence. In this broad sense there are several coefficients, measuring the degree of correlation, adapted to the nature of data. A number of different coefficients are used for different situations (Bland, 2000; Sheskin, 2003). The best known is the *Pearson product-moment correlation coefficient*, which is obtained by dividing the covariance of the two variables by the product of their standard deviations using the Eqn 7.5.

$$R(i,j) = \frac{C(i,j)}{\sqrt{C(i,i)C(j,j)}} \tag{7.5}$$

In this context, the null hypothesis asserts that the two variables are not correlated, and the alternative hypothesis asserts that the attributes are correlated.

- Correlation coefficient

  The correlation coefficient r is a measure of the linear relationship between two attributes or columns of data. The value of r can range from -1 to +1 and is independent of the units of measurement. A value of r near 0 indicates little correlation between attributes; a value near +1 or -1 indicates a high level of correlation.

  When two attributes have a positive correlation coefficient, an increase in the value of one attribute indicates a likely increase in the value of the second attribute. A correlation coefficient of less than 0 indicates a negative

correlation. That is, when one attribute shows an increase in value, the other attribute tends to show a decrease.

Consider two variables x and y:

- If r = 1, then x and y are perfectly positively correlated. The possible values of x and y all lie on a straight line with a positive slope in the (x,y) plane.
- If r = 0, then x and y are not correlated. They do not have an apparent linear relationship. However, this does not mean that x and y are statistically independent.
- If r = -1, then x and y are perfectly negatively correlated. The possible values of x and y all lie on a straight line with a negative slope in the (x,y) plane.

In this EEG analysis, MFL and FD data points were determined using step window of 1.6 s, and were fitted using polynomial fit for each session. The error rate corresponding to each session was fitted using same polynomial function. To determine the relation between the changes in MFL with error function, the correlation coefficients were calculated. The correlation coefficients as a measure show the performance of MFL & FD of EEG in relation with the level of alertness.

7.3.3 Observations - Performance of Fractal features (MFL and FD) to measure alertness level

Fig.7.6 and Fig.7.7 show the polynomial fit plot of MFL, FD and error rate function of two channels (Channel 1 and Channel 3) for experimental session

no.3654. It is observed from the plot that, as error rate increases the MFL decreases, which relates to the indication of the alertness level. The correlation between MFL and error rate was measured using the correlation coefficients. The correlation coefficients for different subjects and for different sessions were tabulated in Table 7.8.

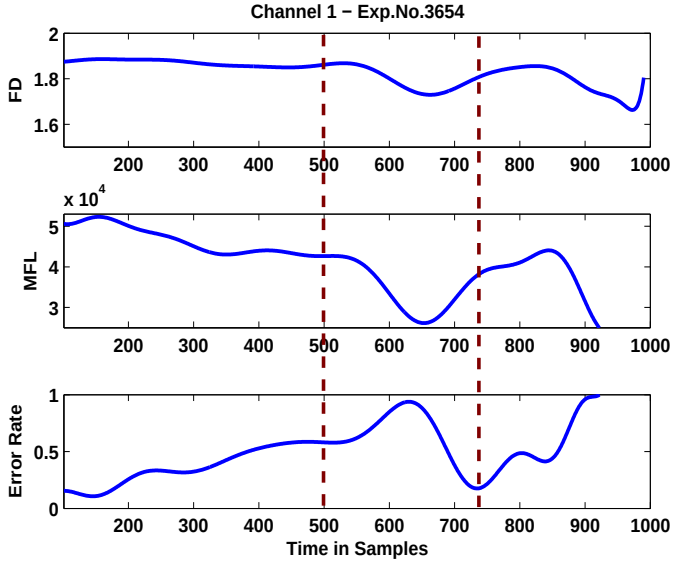

Figure 7.6: Plot of FD and MFL (Channel 1 during session no. 3654) inversely correlated with the local error rate using polynomial fit

7.3.3.1 Correlation coefficients of MFL with Error rate

The correlation coefficients determines how well the MFL of EEG is correlated with the error rate. The correlation coefficients were calculated using correlation analysis. The negative correlation coefficients between the MFL and FD with local error rate function is shown in Table 7.8 and Table 7.9 respectively.

The negative correlation coefficients indicate that MFL is linearly and inversely correlated with the corresponding error rate. From the Table 7.8, it is

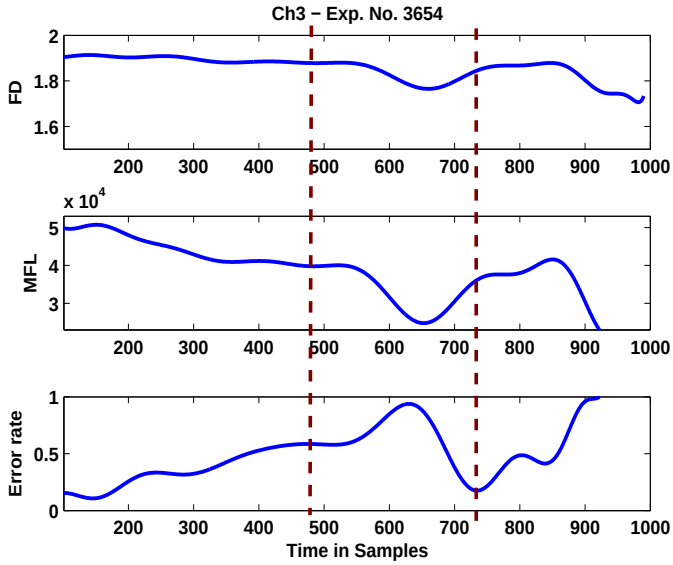

Figure 7.7: Plot of FD and MFL (Channel 3 during session no. 3654) inversely correlated with the local error rate using polynomial fit

Table 7.8: Negative correlation coefficients for MFL and local error rate

Experiment Nos	Negative Correlation coefficient	
	Channel 1	Channel 3
Subject A - No.3648	0.8183	0.834
- No.3674	0.821	0.8023
Subject B - No.3654	0.857	0.8251
- No.3656	0.8442	0.8129
Subject C - No.3665	0.7934	0.8014
- No.3673	0.7842	0.7925

observed that MFL of EEG was negatively correlated (Mean = 0.8196 and SD = 0.02810) with corresponding local error rate to determine the alertness levels and shows that MFL of EEG reliably identified the small changes related with the fluctuations of the subject's task performance and putative alertness level. The results indicate that with only two EEG channels, the MFL of EEG changes with

the changes in alertness level of the subjects with the mean correlation coefficent of 0.82.

Table 7.9: Negative correlation coefficients for FD and local error rate

Experiment Nos	Negative Correlation coefficient	
	Channel 1	Channel 3
Subject A - No.3648	0.7031	0.724
- No.3674	0.691	0.713
Subject B - No.3654	0.656	0.622
- No.3656	0.664	0.6792
Subject C - No.3665	0.6414	0.6258
- No.3673	0.6325	0.6436

It has been demonstrated by (Jung et al., 1997; Makeig et al., 1996) that there is a change in the strength of EEG with change in alertness. This study has identified MFL as a feature that correlates with the strength of the EEG signal. The changes in the level of the alertness can vary the level of the brain activity and in turn the length of the EEG signal. In this study, the results demonstrate that MFL of EEG decreased as the subject's alertness level is changed. The level of alertness has been recorded in this experiment as the local error rate.

This research study has identified changes in the fractal properties of EEG recordings in response to the changes in alertness of the subject. The performance analysis demonstrates that it is feasible to use fractal features of only two channels of EEG to track an operator's global level of alertness in a sustained-attention task.

7.4 Summary

This chapter has reported on the performance analysis of fractal features of biosignals like sEMG, EEG in identification of small changes in activity. This analysis results has demonstrated that the combined use of FD and MFL for a single channel sEMG in identifying finger and wrist flexion actions where the level of contractions is small and when multiple muscles are simultaneously active. The results of this analysis show that in comparison, RMS of the signal is unable to reliably identify the actions, even if more number of channels (2 and 4) were to be used. There was no observable impact of inter-experimental variations on the efficacy of the use of FD and MFL of single channel sEMG to identify the different finger and wrist flexions. Small variations that may have been in the location of electrodes between the placements of electrodes do not appear to have an impact on the ability of the system to accurately identify the different actions.

Based on the experimental outcomes of this study, it is concluded that a combined use of FD and MFL of single channel sEMG is suitable for reliably identifying various finger and wrist flexion actions. The outcomes of this analysis also indicate that the system is not sensitive to inter-experimental variations and does not require strict electrode location selection. This study has also reported the performance analysis of fractal features of EEG to determine or measure the small changes in brain related alertness activities. It is observed that there is a close relationship between the brain activity and the fractal features using only single channel EEG.

Chapter 8

Conclusions

This research work has examined the fractal features of biosignals, mainly sEMG to identify small changes in these kind of signals. This work has demonstrated that using currently available techniques, this can be unreliable due to the presence of other similar signals and noise. Based on the analysis of the fractal properties of the signals, this thesis has developed a new biosignal classification paradigm which is based on the fractal features. This paradigm has been applied successfully to identify subtle finger and wrist movements using sEMG recorded from the forearm. This tecnique has also been successfully applied on electroencephalogram(EEG) signals to measure alertness levels.

The self-similar property of sEMG was analysed in this study and in turn has confirmed the fractal nature of sEMG when the muscles are weakly active. A new fractal based feature - Maximum Fractal length (MFL) of sEMG has been identified which is closely related to the strength of the muscle activation even when the strength of muscle contraction is very small. The experimental results demonstrate that MFL is a much better measure of strength of muscle contraction compared with root mean square (RMS), a common feature in measuring strength of muscle contraction. The performance of MFL was demonstrated for

its abilitiy to identify small changes in muscle activity. Statistical comparison of the relationship of MFL and RMS with strength of contraction indicates that MFL is a significantly better measure of muscle activity than RMS for all levels of muscle contraction. When the level of contraction is less than or equal to 50%, RMS does not appear to be a good measure of contraction ($p < 0.05$) while MFL is a good measure even when the strength of contraction is only 20% MVC ($p < 0.001$).

This work has concluded that Fractal dimension (FD) is dependent on the muscle properties- with larger and more complex muscles having a higher FD. It has also been observed that FD is higher when there are multiple active muscles. Based on the experimental results and theoretical reasoning, this research has concluded that the observed change in FD with change in strength of muscle contraction is a result of changes in muscle properties due to high levels of muscle contraction and associated movement or change in length.

This study has also concluded that FD is not dependent on the strength of muscle contraction but on the muscle properties such as size. For small variations in muscle contraction, there is very small change in the value of FD ($\approx 1\%$) while there is a significant change in MFL ($\approx 200\%$). The study has also demonstrated that FD is dependent on the size and complexity of the active muscles, with the value of FD being higher for larger muscles, or when there are multiple simultaneously active muscles.

The summarised results of using fractal features - MFL and FD of sEMG :

- MFL is suitable for determining small changes in low level muscle activity. A comparison with RMS of the same data suggests that MFL is a far better measure of strength of muscle contraction than RMS, especially at the lower

levels of contraction.

- FD is based on the complexity of muscle and not on changes in muscle activity.

- The results indicate that using single channel sEMG of forearm, a combination of MFL and FD are suitable for accurately identifying actions resulting from small and complex muscle activity such as wrist and finger flexion.

There are number of applications of being able to identify small changes in muscle activity and to identify the location of the active muscle. Such a system can be used for controlling prosthetic hand for people who may have had their forearm amputated. The lack of sensitivity of the system to the electrode positioning also indicates that this could be used by a lay user, and may also find other applications such as human computer interface for the elderly and for people in special circumstances such as Defence.

This thesis has also reported the results using fractal features on the physiological signals like EEG to determine small changes in brain activity related alertness activities. It is observed that there is a close relationship between the the person's alertness and the fractal features. The results indicate that MFL is negatively correlated with the fluctuations of the subject's task performance and putative alertness level with mean correlation coefficient of 0.82. This research demonstrates that it is feasible to use fractal features of only one channel of EEG to track an operator's global level of alertness during sustained-attention task. This measurement of changes in EEG during other cognitive tasks leads to its applications in bio-medical and brain & cognitive dynamics.

8.1 Main Contributions of this thesis

The following presents the main contributions of this thesis:

- This thesis has established that changes in FD of sEMG are attributable to the size and complexity of the muscle and not to the muscle activation.
- It has been demonstrated that there is a strong relationship between the MFL and low level muscle activity. This has been experimentally verified. Statistical analysis has shown that the class separation was much better when MFL was used than RMS. This was validated using the recorded finger flexions with various measured force.
- It has been demonstrated that FD and MFL of single channel sEMG can be classified to accurately identify the associated finger and wrist flexion. It has also been shown that other features such as RMS of even four channels of sEMG is unable to accurately identify the associated finger and wrist flexions.
- Performance analyses of MFL and FD for EEG were done to measure the level of alertness of the individual while performing sustained attention tasks. The results demonstrated that these features were more accurate than other methods.

8.2 Future studies

While this study has conducted conclusive studies related to fractal analysis of sEMG, there is scope for improved understanding of multifractal analysis when

there are signals of different properties.

There is the need for increased number of subjects and to conduct experiments over a longer period of time to determine the impact of inter-experimental variations. There is the need for conducting flexion and extension while this study has only studied the flexion. It is envisaged that this would require two sets of electrodes.

This technique could also find applications in other fields such as related to audio. One future direction could be to test the efficacy of this technique for audio related applications to identify the background and the foreground activity. This technique could be combined with blind source separation to have better outcomes when there are multiple active sources, which can be an another option for future studies.

References

Accardo, A., Affinito, M., Carrozzi, M. and Bouquet, F. (1997), 'Use of the fractal dimension for the analysis of electroencephalographic time series.', *Biological cybernetics* **77**(5), 339–350. 102

Acharya, Bhat, S. P., Kannathal, N., Rao, A. and Lim, C. M. (2005), 'Analysis of cardiac health using fractal dimension and wavelet transformation', *ITBM-RBM* **26**(2), 133–139. 13, 54

Akujuobi, C. and Baraniecki, A. (1992), 'Wavelets and fractals: a comparative study', *Statistical Signal and Array Processing, 1992. Conference Proceedings., IEEE Sixth SP Workshop on* pp. 42–45. 37

Anmuth, C. J., Goldberg, G. and Mayer, N. H. (1994), 'Fractal dimension of electromyographic signals recorded with surface electrodes during isometric contractions is linearly correlated with muscle activation', *Muscle & Nerve* **17**(8), 953–954. 4, 13, 14, 43, 54

Barisi, N. (2007), 'The adaptive ARMA analysis of EMG signals', *Journal of Medical Systems* **32**(1), 43–50. 10

Basmajian, J. and De Luca, C. J. (1985), *Muscles Alive: Their Functions Revealed*

by Electromyography., fifth edn, Williams & Wilkins, Baltimore, MD. 1, 3, 4, 9, 10, 14, 18, 19, 20, 22, 24, 27, 54, 66, 68

Bassingthwaighte, J., Liebovitch, L. and West, B. (1994), *Fractal Physiology*, New York: Oxford University Press. 40, 43, 47

Beckers, F., Verheyden, B., Couckuyt, K. and Aubert, A. E. (2006), 'Fractal dimension in health and heart failure.', *Biomedizinische Technik. Biomedical engineering* **51**(4), 194–197. 102

Bland, M. (2000), *An Introduction to Medical Statistics*, third edn, Oxford University Press. 106

Bourke, P. (2007), 'Self similarity', *Fractals, Chaos* .
URL: *http://local.wasp.uwa.edu.au/ pbourke/fractals/selfsimilar/* xvi, 39, 40, 41, 42, 47

Bullock, T. H., McClune, M. C., Achimowicz, J. Z., Iragui-Madoz, V. J., Duckrow, R. B. and Spencer, S. S. (1995), 'Temporal fluctuations in coherence of brain waves.', *Proceedings of the National Academy of Sciences of the United States of America* **92**(25), 11568–11572. 102

Chambers, J., Cleveland, W., Kleiner, B. and Tukey, P. (1983), *Graphical Methods for Data Analysis*, Wadsworth and Brooks/Cole. 71

Chang, Y.-W., Su, F.-C., Wu, H.-W. and An, K.-N. (1999), 'Optimum length of muscle contraction,', *Clinical Biomechanics* **14**(8), 537–542. 64

Chapotot, F., Gronfier, C., Jouny, C., Muzet, A. and Brandenberger, G. (1998), 'Cortisol secretion is related to electroencephalographic alertness in human

subjects during daytime wakefulness.', *The Journal of clinical endocrinology and metabolism* **83**(12), 4263–4268. 102

Chen, B. and Wang, N. (2000), Determining EMG embedding and fractal dimensions and its application, *in* 'Engineering in Medicine and Biology Society, 2000. Proceedings of the 22nd Annual International Conference of the IEEE', Vol. 2, pp. 1341–1344. 46

Christodoulou, C. I. and Pattichis, C. S. (1999), 'Unsupervised pattern recognition for the classification of emg signals', *Biomedical Engineering, IEEE Transactions on* **46**(2), 169–178. 3, 10

Coatrieux, J. L., Toulouse, P., Rouvrais, B. and Bars, R. L. (1983), 'Automatic classification of electromyographic signals', *EEG Clin. Neurophysiol.,* **55**, 333–341. 3, 10

Costanza, E., Inverso, S. A. and Allen, R. (2005), Toward subtle intimate interfaces for mobile devices using an EMG controller, *in* 'CHI '05: Proceedings of the SIGCHI conference on Human factors in computing systems', ACM Press, New York, NY, USA, pp. 481–489. 35, 88, 92

Cram, J., Kasman, G. and Holtz, J. (1998), *Introduction to Surface Electromyography*, Aspen Publishers, Inc., Gaithersburg, Maryland. 3, 5, 20, 21, 22, 26, 27, 28

Crawford, B., Miller, K., Shenoy, P. and Rao, R. (2005), Real-time classification of electromyographic signals for robotic control, Technical report, University of Washington. 2, 4, 11

De Luca, C. (2006), *Electromyography*, Encyclopedia of Medical Devices and Instrumentation, John Wiley Publisher, pp. 98–109. xv, 26, 27, 29, 30

Devaney, R. L. (1995), 'Chaos in the classroom', *Mathematics and Statistics at Boston University* .
URL: *http://math.bu.edu/DYSYS/chaos-game/chaos-game.html* 10, 44

Duchêne, J. and Goubel, F. (1993), 'Surface electromyogram during voluntary contraction: processing tools and relation to physiological events', *Crit Rev Biomed Eng* **21**(4), 313–397. 4, 8, 9

Durgam, V., Fernandes, G., Preiszl, H., Lutzenberger, W., Pulvermuller, F. and Birbaumer, N. (1997), 'Fractal dimensions of short eeg time series in humans', *Neuroscience Letters* **225**(2), 77–80. 49, 102

Englehart, K. and Hudgins, B. (2003), 'A robust, real-time control scheme for multifunction myoelectric control', *IEEE Transactions on Biomedical Engineering* **50**(7), 848–854. 1, 3, 9, 11

Esteller, R., Vachtsevanos, G., Echauz, J. and Litt, B. (2001), 'A comparison of waveform fractal dimension algorithms', *Circuits and Systems I: Fundamental Theory and Applications, IEEE Transactions on [see also Circuits and Systems I: Regular Papers, IEEE Transactions on]* **48**(2), 177–183. 50, 51

Falconer, K. (1990), *Fractal Geometry - Mathematical Foundations and Applications*, John Wiley and Sons, New York. 37, 43

Falla, D., Farina, D. and Graven-Nielsen, T. (2007), 'Spatial dependency of

trapezius muscle activity during repetitive shoulder flexion', *Journal of electromyography and kinesiology* **17**(3), 299–306. 88

Farina, D., Merletti, R. and Stegeman, D. F. (2005), *Biophysics of the Generation of* EMG *Signals*, Electromyography, Wiley-IEEE Press, pp. 81–105. 21, 22, 28, 34

Feder, J. (1988), *Fractals*, New York: Plenum Press. 39, 40, 43, 47

Fisher, R. A. (1922), 'On the interpretation of χ^2 from contingency tables, and the calculation of p', *Journal of the Royal Statistical Society* **85**(1), 87–94. 94

Freeman, A. and Skapura, M. (1991), *Neural Networks : Algorithms, Applications and Programming Techniques*, Addison-Wesley. 96

Fridlund, A. J. and Cacioppo, J. T. (1986), 'Guidelines for human electromyographic research', *Psychophysiology* **23**(5), 567–589. 66

Gazzoni, M., Farina, D. and Merletti, R. (2004), 'A new method for the extraction and classification of single motor unit action potentials from surface emg signals', *Journal of Neuroscience Methods* **136**, 165–177. 4, 5

Gitter, J. A. and Czerniecki, M. J. (1995), 'Fractal analysis of the electromyographic interference pattern', *Journal of Neuroscience Methods* pp. 103–108. 4, 12, 13, 14, 52, 54, 60

Goldberger, A. L., Amaral, L. A. N., Glass, L., Hausdorff, J. M., Ivanov, P. C., Mark, R. G., Mietus, J. E., Moody, G. B., Peng, C.-K. and Stanley, H. E. (2000), 'PhysioBank, PhysioToolkit, and PhysioNet: Components of a new research resource for complex physiologic

signals', *Circulation* **101**(23), e215–e220. Circulation Electronic Pages: http://circ.ahajournals.org/cgi/content/full/101/23/e215. 39, 43, 45, 46, 47

GraphPad (2007), 'How the f test works to compare models', *GraphPad Prism 5.0 Software: Learning module* . 94

Graupe, D. and Cline, W. K. (1975), 'Functional separation of SEMG signals via arma identification methods for prosthesis control purposes', *IEEE Transaction on Systems, Man, and Cybernetics* **5**(2), 252–259. 17

Green, E. R. (1998), 'Understanding fractals and fractal dimensions', *Senior Honor Thesis - University of Wisconsin, Madison, WI* .
URL: *http://pages.cs.wisc.edu/ẽrgreen/honors_thesis/similar.html* xvi, 37, 38

Grigg-Damberger, M., Gozal, D., Marcus, C. L., Quan, S. F., Rosen, C. L., Chervin, R. D., Wise, M., Picchietti, D. L., Sheldon, S. H. and Iber, C. (2007), 'The visual scoring of sleep and arousal in infants and children.', *Journal of clinical sleep medicine : JCSM : official publication of the American Academy of Sleep Medicine* **3**(2), 201–240. 102

Gupta, V., Suryanarayanan, S. and Reddy, N. P. (1997), 'Fractal analysis of surface EMG signals from the biceps', *International Journal of Medical Informatics* pp. 185–192. 4, 12, 13, 14, 43, 49, 52, 54, 55, 60

Hair, J. F., Black, W. C., Babin, B. J., Anderson, R. E. and Tatham, R. L. . (2006), *Multivariate Data Analysis*, Prentice Hall. 94, 95

Henneman, E., Somjem, G. and Carpenter, D. (1965), 'Functional organization of cell size in spinal motoneurons', *Journal of Neurophysiology* **28**, 560–580. 20

Hermens, H. J., Freriks, B., Disselhorst-Klug, C. and Rau, G. (2000), 'Development of recommendations for SEMG sensors and sensor placement procedures', *Journal of Electromyography and Kinesiology* **10**(5), 361–374. 66

Higuchi, T. (1988), 'Approach to an irregular time series on the basis of the fractal theory', *Phys. D* **31**(2), 277–283. 50, 51

Holobar, A. and Zazula, D. (2003), 'Surface EMG decomposition using a novel approach for blind source separation', *Informatica Medica Slovenica* **8**, 2–14. **URL:** *http://storm.uni-mb.si/semg/* 55

Hu, X., Wang, Z. Z. and Ren, X. M. (2005), 'Classification of surface EMG signal with fractal dimension.', *Journal of Zhejiang University - Science. B* **6**(8), 844–848. 4, 13, 14, 52, 60

Huang, H.-P. and Chen, C.-Y. (1999), 'Development of myoelectric discrimination system for a multi-degree prosthetic hand', *IEEE International Conference on Robotic and Automation* . 18

Huiskamp, G.-J., Blok, J., Stegeman, D. and Houtman, C. (1995), 'An estimation procedure to determine motor unit structure from surface EMG data', *Electroencephalography and Clinical Neurophysiology/ Electromyography and Motor Control* **97**, 166–166(1). 55

Iannaconne, P. and Khokha, M. (1996), *Fractal Geometry in Biological Systems: An Analytical Approach*, Boca Raton: CRC Press. 40

Ivanov, P. C., Amaral, L. A. N., Goldberger, A. L. and Stanley, H. E. (1998),

'Stochastic feedback and the regulation of biological rhythms', *EPL (Europhysics Letters)* **43**(4), 363–368. 45

Jung, T.-P., Makeig, S., Stensmo, M. and Sejnowski, T. J. (1997), 'Estimating alertness from the eeg power spectrum', *Biomedical Engineering, IEEE Transactions on* **44**(1), 60–69. 102, 103, 110

Kalden, R. and Ibrahim, S. (2004), Searching for self-similarity in gprs, *in* 'PAM 2004 : Passive and Active network Masurement', pp. 83–92. 41

Karlsson, S., Yu, J. and Akay, M. (2000), 'Time-frequency analysis of myoelectric signals during dynamic contractions: a comparative study', *Biomedical Engineering, IEEE Transactions on* **47**(2), 228–238. 8, 10

Katsis, C. D., Exarchos, T. P., Papaloukas, C., Goletsis, Y., Fotiadis, D. I. and Sarmas, I. (2007), 'A two-stage method for muap classification based on EMG decomposition', *Computers in Biology and Medicine* **37**(9), 1232–1240. 3

Katz, M. J. (1988), 'Fractals and the analysis of waveforms.', *Computers in biology and medicine* **18**(3), 145–156. 50

Kleine, B. U., van Dijk, J. P., Lapatki, B. G., Zwarts, M. J. and Stegeman, D. F. (2007), 'Using two-dimensional spatial information in decomposition of surface EMG signals', *Journal of electromyography and kinesiology : official journal of the International Society of Electrophysiological Kinesiology* **17**(5), 535–548. 3, 4, 10, 46, 55

Knox, R. and Brooks, D. (1994), 'Classification of multifunction surface emg using

advanced ar model representations', *Proceedings of the 20th Annual Northeast Bioengineering Conference* pp. 96–98. 10

Kobayashi, M. and Musha, T. (1982), '1/f fluctuation of heartbeat period', *Biomedical Engineering, IEEE Transactions on* **BME-29**(6), 456–457. 44

Kumar, D. K., Ma, N. and Burton, P. (2001), 'Classification of dynamic multi-channel electromyography by neural network', *Electromyography and Clinical Neurophysiology* **41**(7), 401–408. 3, 10

Kumar, D. and Pah, N. D. (2000), 'Neural networks and wavelet decomposition for classification of surface electromyography', *Electromyography and Clinical Neurophysiology* **40**(6), 411–421. 3, 10, 27

Lévy-Véhel, J. and Lutton, E. (2006), *Fractals in Engineering; New Trends in Theory and Applications*, Springer-Verlag New York, Inc., Secaucus, NJ, USA. 43

Lomax, R. G. (2001), *An Introduction to Statistical Concepts for Education and Behavioral Sciences*, second edn, Lawrence Erlbaum Associates. 94

Lowery, M. M. and O'Malley, M. J. (2003), 'Analysis and simulation of changes in EMG amplitude during high-level fatiguing contractions', *Biomedical Engineering, IEEE Transactions on* **50**(9), 1052–1062. 46, 88

Makeig, S. and Inlow, M. (1993), 'Lapses in alertness: coherence of fluctuations in performance and eeg spectrum.', *Electroencephalography and clinical neurophysiology* **86**(1), 23–35. 102

Makeig, S., Jung, T.-P. and Sejnowski, T. J. (1996), 'Using feedforward neural networks to monitor alertness from changes in eeg correlation and coherence.', *Advances in Neural Information Processing Systems* **8**, 931–937. 103, 110

Mandelbrot, B. B. (1977), *Fractals: Form, chance, and dimension*, first edn, W. H. Freeman and Co.,, San Francisco. 13, 14, 36, 37, 43, 54

Marieb, E. N. (1997), *Human Anatomy and Physiology*, fourth edn, Benjamin/Cummings publishing, Addison wesley, California. 31, 32, 64, 74, 75, 89

Merletti, R. (2008), '**EMG**', *DEMUSE* .
URL: *http://www.lisin.polito.it/DEMUSE/Publish/EMGs.html* xv, 19, 22, 23

Merletti, R., Rainoldi, A. and Farina, D. (2005), *Myoelectric manifestations of muscle fatigue*, Electromyography, Wiley-IEEE Press, pp. 233–253. 9

Momen, K., Krishnan, S. and Chau, T. (2007), 'Real-time classification of forearm electromyographic signals corresponding to user-selected intentional movements for multifunction prosthesis control', *Neural Systems and Rehabilitation Engineering, IEEE Transactions* **15**(4), 535–542. 1, 2, 9, 11, 92, 96

Moritani, T., Stegeman, D. F. and Merletti, R. (2005), *Basic Physiology and Biophysics of* EMG *signal generation*, Electromyography, Wiley-IEEE Press, pp. 1–25. 18

Nagata, K., Adno, K., Magatani, K. and Yamada, M. (2005), 'A classification method of hand movements using multi channel electrode', *27th Annual In-*

ternational Conference of the Engineering in Medicine and Biology Society pp. 2375–2378. xv, 2, 4, 9, 10, 12

Nagata, K. and Magatani, K. (2004), 'Development of the assist system to operate a computer for the disabled using multichannel surface EMG', *Proceedings of 26th Annual International conference of the IEEE Engineering in Medicine and Biology Society* . 9

Nussbaum, M. A. (2006), 'Localized muscle fatigue', *Lecture Notes on Advanced Methods in Occupational Biomechanics* .
URL: *http://www.nussbaum.org.vt.edu/courses.htm* 5, 11

Osamu Fukuda, T. T. (2004), 'Control of an externally powered prosthetic forearm using raw-EMG signals', *SICE* **40**(11), 1124–1131. 9

Palastanga, N., Field, D. and Soames, R. (2006), *Anatomy and Human movement: structure and function*, fifth edn, Butterworth-Heinemann, Elsevier, Philadelphia. xv, 32, 33, 58, 64, 74, 75, 89

Paramanathan, P. and Uthayakumar, R. (2008), 'Application of fractal theory in analysis of human electroencephalographic signals.', *Computers in biology and medicine* **38**(3), 372–378. 102

Peng, C.-K., Hausdorff, J. and Goldberger, A. (1999), 'Fractal mechanisms in neural control: Human heartbeat and gait dynamics in health and disease.', *Nonlinear Dynamics, Self-Organization, and Biomedicine* . 44, 45, 49

Petrosian, A. (1995), Kolmogorov complexity of finite sequences and recognition

of different preictal eeg patterns, *in* 'Computer-Based Medical Systems, 1995., Proceedings of the Eighth IEEE Symposium on', pp. 212–217. 50

Rainoldi, A., Casale, R., Hodges, P. and Jull, G. (2005), *Applications in rehabilitation medicine and related fields*, Electromyography, Wiley-IEEE Press, pp. 403–425. 9

Ren, X. H., Wang, Z. and Yan, Z. (2006), 'Muap extraction and classification based on wavelet transform and ICA for EMG decomposition', *Medical and Biological Engineering and Computing* **44**, 371–382. 3, 4, 10

Sandbrink, F. and Culcea, E. (2002), *Motor Unit Recruitment in* EMG. 3, 23

Sarkar, M. and Leong, T.-Y. (2003), 'Characterization of medical time series using fuzzy similarity-based fractal dimensions', *Artificial Intelligence in Medicine* **27**(2), 201–222. 43

ShadowRobot (2008), 'Shadow hand', *Shadow Robot Company Ltd* .
URL: *http://www.shadowrobot.com/* xv, 2

Sheskin, D. (2003), *Handbook of Parametric and Nonparametric Statistical Procedures*, third edn, CRC Press. 106

Silber, M. H., Ancoli-Israel, S., Bonnet, M. H., Chokroverty, S., Grigg-Damberger, M. M., Hirshkowitz, M., Kapen, S., Keenan, S. A., Kryger, M. H., Penzel, T., Pressman, M. R. and Iber, C. (2007), 'The visual scoring of sleep in adults.', *J Clin Sleep Med* **3**(2), 121–131. 102

Stashuk, D. (2001), 'EMG signal decomposition: how can it be accomplished and used?', *Journal of Electromyography and Kinesiology* **11**(3), 151–173. 10

Tassi, P., Bonnefond, A., Engasser, O., Hoeft, A., Eschenlauer, R. and Muzet, A. (2006), 'Eeg spectral power and cognitive performance during sleep inertia: the effect of normal sleep duration and partial sleep deprivation.', *Physiology & behavior* **87**(1), 177–184. 102

TekscanInc (2007), 'Specs-flexiforce', *Flexiforce Sensor* .
URL: *http://www.tekscan.com/flexiforce/specs-flexiforce.html* xvi, 68

Tsuji, T. and Kaneko, M. (2000), 'An EMG controlled pointing device using a neural network', *SICE* **37**(5), 425–431. 9

Venturini, R., Lytton, W. and Sejnowski, T. (1992), 'Neural network analysis of event related potentials and electroencephalogram', *Advances in Neural Information Processing Systems* **4**, 651–658. 103

Xu, Z. and Xiao, S. (1997), Fractal dimension of surface EMG and its determinants, *in* 'Engineering in Medicine and Biology Society, 1997. Proceedings of the 19th Annual International Conference of the IEEE', Vol. 4, pp. 1570–1573 vol.4. 13

Zhonggang, L. and Hong, Y. (2006), 'A method to estimate the short-term fractal dimension of heart rate variability based on wavelet transform', *Journal of biomedical engineering* **23**(5), 981–985. 102

Zhou, P. and Rymer, W. Z. (2007), 'Muap number estimates in surface EMG: Template - matching methods and their performance boundaries', *Computers in Biology and Medicine* **32**, 1007–1015. 3

Zhou, P., Rymer, W. Z., Suresh, N. and Zhang, L. (2001), 'A study of surface motor unit action potentials in first dorsal interosseus (fdi) muscle', *23rd Annual International Conference of the IEEE Engineering in Medicine and Biology Society* **2**, 1074–1077. 3